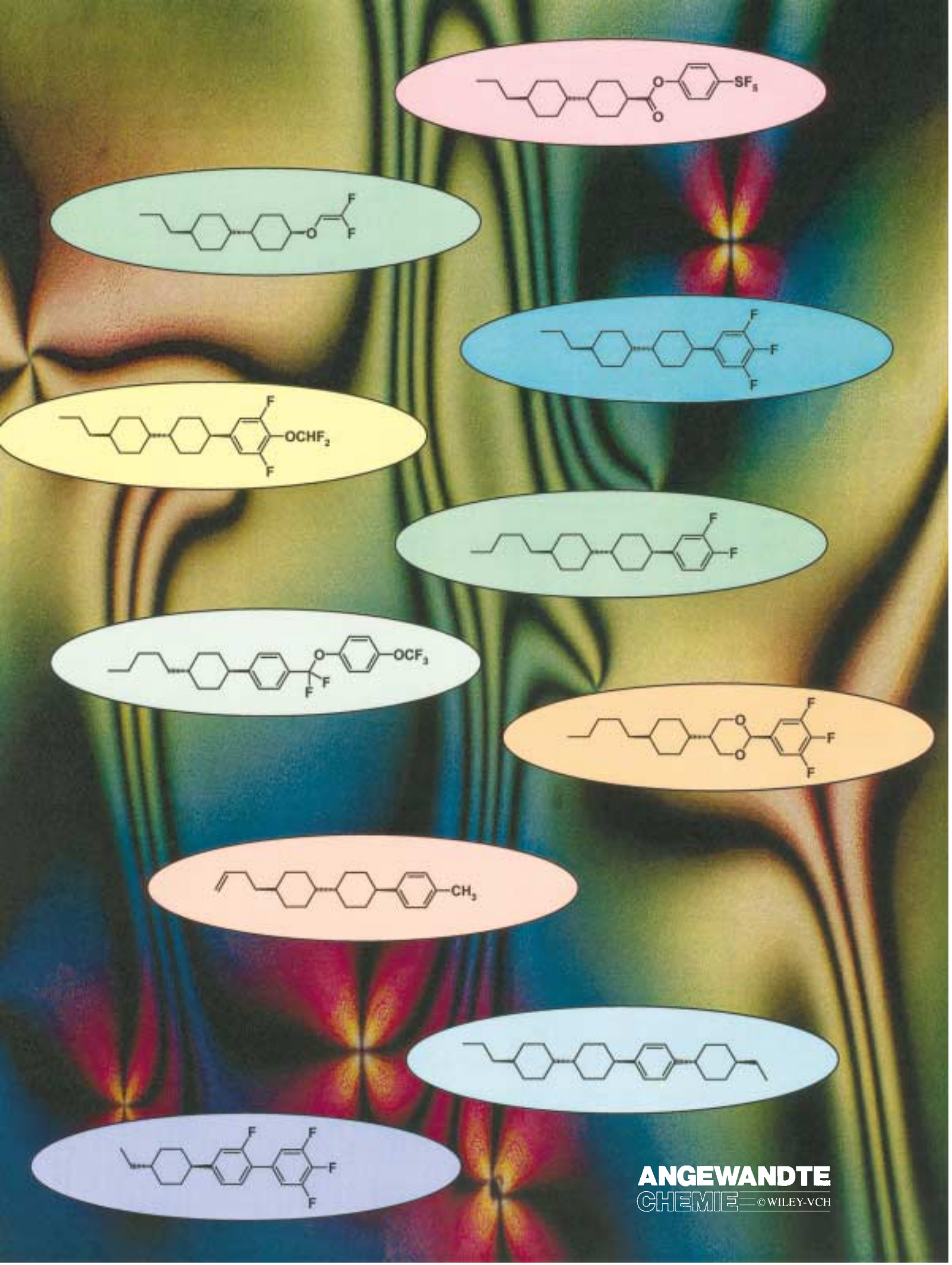

ANGEWANDTE
CHEMIE

Nematic Liquid Crystals for Active Matrix Displays: Molecular Design and Synthesis**

Peer Kirsch* and Matthias Bremer*

Substances forming calamitic mesophases have been known for more than 100 years but only the recent, rapid advance in active matrix liquid crystal display (AM-LCD) technology helped these materials to achieve the crucial position in flat panel display technology they hold today. Due to their high contrast, large viewing angle, and rapid switching times, modern AM-LCDs offer a superior picture quality even compared to conventional cathode ray tubes. Their flatness, low weight, and low energy consumption render them the technology of choice for all kinds of portable devices. Some of the future promises of AM-LCD technology are centered around the development of liquid crystalline materials for the different subtypes of active matrix applications. This development is aimed, on the one hand, towards improved electrooptical and viscoelastic properties; on the other hand, the increasing performance of LCDs leads to extremely stringent reliability demands on the liquid crystals. Responding to these high standards of performance and quality, most liquid crystals for contemporary AM-LCD applications are multiply fluorinated compounds with very high purities, as is typical for materials used in the electronics industry. The synthesis of these superfluorinated materials (SFMs) often requires specialized methods, which, in several cases, had to be introduced for the first time into the canon of industrial production. The immense market pressure, as well as the rapid advance of AM-LCD technology on the side of the display manufacturers, urges an increasing pace of the materials development. This demand for new materials can no longer be fulfilled by conventional trial-and-error approaches. As in the pharmaceutical industry, in the search for new, superior liquid crystals, the purely empirical methods are increasingly supported by a rational design based on computational methods.

Keywords: fluorine chemistry · liquid crystals · mesogens · metallation · molecular modeling

1. Introduction

In the past few years, liquid crystal displays (LCD) have become a nearly inseparable part of our daily life. In 1999, more than two billion LCDs were produced worldwide;[1] half of them small monochrome displays for watches and video games. A smaller but rapidly growing fraction of this overall number are full-color displays capable of high-resolution graphics. Perhaps the most prominent example for this type of high information content display are the desktop computer monitors (about 3.6 million units produced in 1999, most of them with a 15" (37.5 cm) diagonal screen), which have started to compete seriously with the long-established cathode ray tube (CRT) monitors. Having overcome some of the major obstacles on the way to larger panel sizes, display manufacturers are now targeting the "hang-on-the-wall" flat-screen TV as their next strategic goal, which will surely be accomplished within the first half of the next decade.

Most of these high-end displays are based on the active matrix (AM) technology,[2, 3] where each picture element ("pixel") is controlled separately by a thin film transistor (TFT) integrated on the panel glass. The principle components of an LCD are the glass substrate, covered by an indium tin oxide (ITO) layer as transparent electrode material, polarizer and birefringent compensator films, and color filters. The "heart" of most commercial LCDs is a 5–6 μm thick film of a nematic liquid crystal. The apparently quite small world production volume of liquid crystals (about 55 t in 1999)[4] is easily explained by the fact that most LCDs require only 0.5–

[*] Dr. P. Kirsch, Dr. M. Bremer
Merck KGaA, Liquid Crystals Division
64271 Darmstadt (Germany)
Fax: (+49) 6151-722593
E-mail: peer.kirsch@merck.de, matthias.bremer@merck.de

[**] A part of the work reviewed in this article was performed under the management of the Association of Super-Advanced Electronics Industries (ASET) in the R&D program of the Japanese Ministry of International Trade and Industry (MITI) with support from the New Energy and Industrial Development Organization (NEDO). Another part was supported by the German Bundesministerium für Bildung und Forschung (01 B 621/1).

  1433-7851/00/3923-4217 $ 17.50+.50/0

0.6 mg of liquid crystal per square centimeter. Currently around 40 % of the worldwide liquid crystal production is used for AM-LCDs.

The broad application of liquid crystal displays became feasible when, in 1971, the twisted–nematic (TN) cell was invented by Schadt and Helfrich.[5] In a liquid crystal cell based on the TN mode, a nematic liquid crystalline material, with positive dielectric anisotropy ($\Delta\varepsilon$) and helically twisted by 90°, is placed in an ITO lined glass cell and arranged in an homogeneously aligned layer (that is, parallel to the glass) between crossed polarizers (Figure 1).[6–12] The orientation of the liquid crystal is achieved by an alignment layer of directionally rubbed polyimide within the cell. In order to ensure a homogeneous handedness of the helical structure and, thus, to avoid the formation of domains in the display, a small amount (up to 0.1 %) of a chiral dopant is added to the liquid crystal material.[13] In the off state, the incoming light is polarized and the polarization plane of the light passing through the liquid crystal layer is rotated by 90° and is thus able to exit the second polarizer. If an electrical potential is applied, the liquid crystal helix is deformed and the incoming light cannot pass the crossed polarizers. Thus, in the off state, the cell, which is illuminated from the back, appears white; in the on state, black. A grey scale can be achieved by applying a voltage between the threshold voltage (V_{th}) and the saturation voltage.

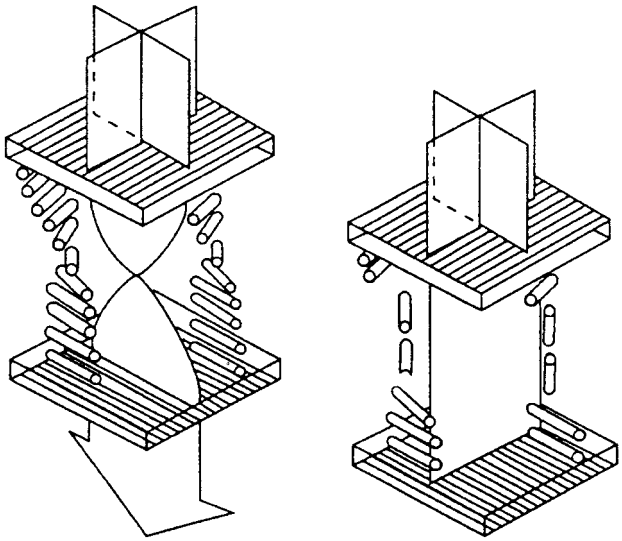

Figure 1. Schematic representation of the working principle of a TN cell in the off (left) and on (right) states. Reproduced from ref. [2] with permission.

At the early 1970s, Gray and co-workers[14] synthesized the first chemically and photochemically stable liquid cystals that exhibited a nematic phase at room temperature (**1**, Scheme 1). Another commercially important new class of materials also

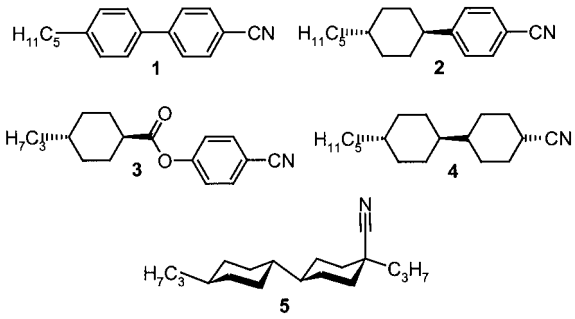

Scheme 1. Examples of the first chemically stable liquid crystals which have a nematic phase around room temperature.

M. Bremer P. Kirsch

Peer Kirsch was born in Herford, Germany, in 1965. He studied chemistry at Heidelberg University and received his Ph.D. early in 1993 under the supervision of Prof. Heinz A. Staab (Max Planck Institute for Medical Research) in physical organic chemistry. After a collaboration with Prof. R. Heiner Schirmer (Heidelberg University) on flavin-based enzyme inhibitors, he was from 1994 to 1995 on a Feodor Lynen fellowship of the Alexander von Humboldt Foundation and a fellowship of the Japanese Science and Technology Agency (STA) at the Institute of Physical and Chemical Research (RIKEN) in Wako, Saitama. There he worked with Prof. Tomoya Ogawa in the field of carbohydrate chemistry. He joined the Liquid Crystal Division of Merck KGaA in November 1995. His main research interest is the application of fluorine chemistry for the design and synthesis of liquid crystals.

Matthias Bremer received his "Diplom-Chemiker" from the Erlangen University in 1986 and a Ph.D. degree from the same institution in 1989. In Erlangen, his work was on physical organic chemistry under the supervision of Prof. Paul von Ragué Schleyer. From late 1989 until December 1990 he was a Feodor Lynen fellow of the Alexander von Humboldt Foundation at the University of California in Berkeley, where he studied chiral organometallic compounds with Prof. Andrew Streitwieser. He joined Merck KGaA in early 1991 and has worked in the Liquid Crystal research department since. In addition to a number of patents, he has published some 30 research papers on computational chemistry, synthetic and physical organic chemistry, X-ray crystallography, and liquid crystals.

with a nematic phase around ambient temperature, the cyanophenylcyclohexanes (**2**), were introduced by Eidenschink[15] in 1977. By systematically utilizing the melting point depression of mixtures of these and similar materials,[16–19] it was possible to produce TN-LCDs with a reasonable working temperature range and, in principle, an unlimited lifetime.[20] Soon, the range of commercially applicable liquid crystalline materials was further broadened by other cyano based compounds.

The first TN-LCDs were simple, directly addressed segment displays, as still used today in wrist watches, for example. In attempting to increase the information content of the displays, by time-sequential addressing in rows and lines, the limits of the TN cell were soon met: At higher multiplex ratios,[21] a severe loss in contrast occurred due to the ever shorter addressing times. The development of the super-twisted nematic (STN) cell in 1984[22] pushed the practicable limit to higher multiplex ratios but did not lead to a general solution to the problem.

Already at the end of the 1960s, the first commercial LCDs still based on the dynamic scattering mode (DSM)[23, 24] had faced the same principal problem of addressability at higher multiplex ratios. As a solution, the use of an "active matrix" of one thin film transistor (TFT), in combination with a voltage-holding capacitor for each pixel, was proposed.[25–27] In the long term, the DSM mode itself did not prove feasible but the general idea of active matrix addressing was intensively re-evaluated during the 1980s for TN displays,[2] in order to precisely control the applied voltage and thus the optical transmission for each pixel separately. These efforts resulted in the first prototype of a 3" (7.5 cm diagonal) TFT display presented by Sharp in 1986. Since the manufacturing process of the TFT arrays is highly complex and expensive in terms of financial investment and human resources, the larger scale production of AM-LCDs started only 1989 for use in notebook computers.[28]

The major drawback of the first AM-LCDs was the strong dependance of the contrast on the viewing angle, which resulted in grey-scale inversion and color shifts in the display when viewed from any than an approximately perpendicular direction. This problem was solved for the "classic" TN-TFT design by using birefringent compensator films, sometimes in combination with multidomain technology.[29] On the other hand, the last five years showed a technological diversification targeted to further improve the performance of active matrix addressed LCDs: The in-plane switching (IPS) mode[30] and the multidomain vertical alignment (MVA) LCD mode[31] increased the viewing angle to 160° and resulted in a dramatically improved contrast ratio (up to 1:300 for the MVA-LCD). The plasma-addressed LCD (PALC)[32] uses plasma discharges instead of solid state TFTs to address the pixels and allows the design of flat TV screens up to 42" (105 cm) diagonal.

2. Physical Properties of Nematic Liquid Crystals

In order to obtain an optimal performance of any LCD mode, a certain set of physicochemical requirements has to be met by the liquid crystal material. These specifications include, among others, the nematic phase range, dielectric anisotropy ($\Delta\varepsilon$), birefringence (Δn), rotational viscosity (γ_1), and elastic constants (K_1, K_2, K_3).[8, 33–36]

The most basic prerequisite for all types of commercially significant LCDs is surely a broad nematic mesophase range of the liquid crystal. Especially for the rapidly spreading automotive uses, such as car navigation displays, the material must remain stably nematic in a wide temperature range, in many cases from -40 to 110 °C.

In order to respond to an applied switching voltage, a liquid crystal has to exhibit a dielectric anisotropy ($\Delta\varepsilon = \varepsilon_{\parallel} - \varepsilon_{\perp}$),[8, 21, 37] defined as the difference between the dielectric constants parallel and perpendicular to the director of the nematic phase. At the molecular level, $\Delta\varepsilon$ is correlated to the square of the dipole moment μ and to the angle β between the dipole moment vector and the effective orientation axis of the liquid crystal molecule.[38] In order to make Equation (1) useful for the design of materials on an atomistic molecular level and for the prediction of $\Delta\varepsilon$ by computational methods, the orientation axis is usually approximated by the "long molecular axis" (here defined as the rotation axis with the smallest moment of inertia) of the rodlike liquid crystals, even if this leads, in exceptional cases, to inaccurate results.

$$\Delta\varepsilon = \frac{N h F}{\varepsilon_0}\left\{\Delta\alpha - F\frac{\mu^2}{2 k_B T}(1 - 3\cos^2\beta)\right\}S \qquad (1)$$

For the design of liquid crystals, two implications of the Maier–Meier Equation (1)[38] have to be kept in mind: Firstly, independent from the absolute value of the dipole moment μ, at the "magic" angle $\beta = 54.7°$ the contribution from the molecular dipole to $\Delta\varepsilon$ always vanishes, to leave only the very small contribution from $\Delta\alpha$. Secondly, if a local dipole moment is oriented parallel to the orientation axis, it is by a factor of $\sqrt{2}$ as effective in "generating" absolute dielectric anisotropy ($|\Delta\varepsilon|$) than in the case of perpendicular orientation.

The threshold voltage (V_{th}) of the electrooptical response of a dielectrically positive liquid crystal mixture (Figure 2)—and therefore also the driving voltage of a TN display—depends

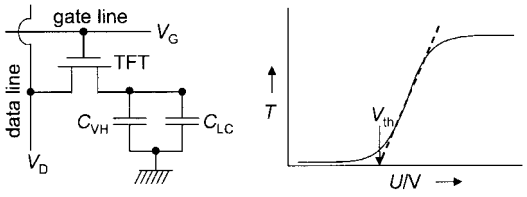

Figure 2. Function of an active matrix liquid crystal display (AM-LCD). Left: the electronic scheme; V_D denotes voltage on the data line, V_G voltage on the gate line, C_{VH} voltage-holding capacitance, C_{LC} capacitance of the liquid crystal layer. Right: the electrooptical response curve of a "normally black" TN cell (parallel polarizers) showing optical transmission T against the applied voltage U; V_{th} denotes the threshold voltage of the electrooptical response.

[Eq. (2)], besides the dielectric anisotropy ($\Delta\varepsilon$), on a set of elastic constants (K_1, K_2, and K_3) also.[21, 37] They describe the

$$V_{th} = \pi\sqrt{\frac{K_1 + \frac{(K_3 - 2K_2)}{4}}{\varepsilon_0\Delta\varepsilon}} \cong \pi\sqrt{\frac{K_1}{\varepsilon_0\Delta\varepsilon}} \qquad (2)$$

different types of elastic deformation of the helical liquid crystal alignment under the influence of an applied electric or magnetic field. Most decisive for TN type cells is the constant K_1, the so-called "splay" deformation.[37]

In order to obtain a good contrast ratio in a display based on the normal TN mode (90° twist, "normally black" mode with parallel polarizers), the relation between the birefringence Δn of the liquid crystal[37] and the cell gap d has to be chosen in a way that in the off state the transmission T, according to the Gooch – Tarry Equation (3), is minimized.[21, 39, 40]

$$T(u) = \frac{1}{2}\frac{\sin^2\left(\frac{\pi}{2}\sqrt{1+u^2}\right)}{1+u^2};\ u = 2d\frac{\Delta n}{\lambda} \qquad (3)$$

For active matrix displays, the first minimum is usually used, to lead to the best viewing angle independence of the picture quality.[41] This arrangement corresponds to a typical birefringence Δn value of 0.0837 for a cell gap of 6 μm. Recently, many display manufacturers are using birefringent compensation films to improve further the viewing angle of the panel. The optical properties of these films have also to be taken into account for the specification of the birefringence of the liquid crystal material. On the molecular level, the birefringence of a nematic liquid crystal mostly depends on the anisotropy of the polarizability ($\Delta\alpha = \alpha_{\parallel} - \alpha_{\perp} = \alpha_{xx} - (\alpha_{yy} + \alpha_{zz})/2$, [Eq. (4)]; the xx axis is the molecular rotation axis with the smallest moment of inertia).[8b, 42]

$$\frac{n_e^2-1}{n^2+2} = \frac{N}{3\varepsilon_0}\left(\alpha+\frac{2\Delta\alpha S}{3}\right);\ \frac{n_0^2-1}{n^2+2} = \frac{N}{3\varepsilon_0}\left(\alpha-\frac{\Delta\alpha S}{3}\right);\ n^2 = \frac{n_e^2+2n_0^2}{3} \qquad (4)$$

For most AMD applications, the switching time has become a decisive factor. The time interval between two video frames at 60 Hz is 16.67 ms. Therefore, multimedia and video applications usually require a fast switching time ($\tau = \tau_{on} + \tau_{off}$; [Eq. (5)])[43] of, at least, less than 20 – 25 ms.

$$\tau_{on} = \frac{\gamma_1 d^2}{\pi^2 K_1\left(\frac{V_{on}^2}{V_{th}^2}-1\right)};\ \tau_{off} = \frac{\gamma_1 d^2}{\pi^2 K_1} \qquad (5)$$

On the materials side, the switching time predominantly depends on the rotational viscosity γ_1,[43] which can vary over a wide range for differently structured liquid crystals. The molecular parameter predominantly influencing γ_1 is the length of the liquid crystal molecule. The "splay" elastic constant K_1 is a far less variable parameter. A theoretical model quantitatively correlating molecular parameters with the viscoelastic parameters of the nematic phase, such as γ_1 or K_1, would be of value but is not available so far. On the side of display design, the switching time can be reduced by a smaller cell gap d. A consequence of this would be the requirement to increase the birefringence Δn of the liquid crystal, according to Equation (3), in order to obtain an optimized viewing angle independence of the contrast. So far, for the larger panel sizes used in notebook, monitor, or TV applications, the reduction of the cell gap, with sufficient accuracy, is technically feasible to about 4.5 μm.

Table 1 shows the most important types of active matrix displays currently in use and their requirements for the physicochemical properties of the liquid crystalline material.

The complex property profile required for the optimum performance of each display type cannot be met by currently existing *single* nematic liquid crystals. The initial task, just to produce a liquid crystal mixture which is nematic around room temperature,[20b] has thus evolved into a multidimensional optimization problem, which is usually approached by mixing 10 to 15 and, sometimes, even more single substances.

In general, the development of nematic liquid crystal mixtures is still based on eutectic "blocks"[20b] of different alkyl homologues of the same classes of materials. Not all components of a liquid crystal mixture have to exhibit a thermodynamically stable nematic phase. Some commonly used materials (for example, the dialkylbicyclohexanes) show only a smectic B (S_B) phase or even no mesophase at all. Nevertheless, if applied in moderate concentrations, they do not induce a smectic phase in the mixture and thus allow

Table 1. Overview over the material requirements for the most important active matrix addressed LCD types.

Technology	Applications	Material Requirements	Characteristics
Standard AM-LCD (5V/4V driver)	PC monitors, notebook computers	$\Delta\varepsilon$ 4 – 6, Δn 0.085 – 0.10, T_{NI} 80 – 120 °C	Well established technology; use of compensation films for improvement of viewing angle independence of contrast
Low V_{th} AM-LCD (3.3V/2.5V driver)	Notebook computers, Personal Digital Assistant (PDA), camera view finders	$\Delta\varepsilon$ 10 – 12, Δn 0.085 – 0.10, $T_{NI} \sim 70$ °C	Allows cheaper and more compact driving electronics than for standard AM-LCD; lower power consumption; very sensitive towards impurities of the liquid crystal material
Reflective TFT	Video games, small notebook computers, PDA	$\Delta\varepsilon$ 4 – 8, Δn 0.06 – 0.07, $T_{NI} \sim 80$ °C	No backlight required, therefore reduction of power consumption by up to ~90 %; relatively low brightness and contrast
In-Plane Switching (IPS)[a]	PC monitors	$\Delta\varepsilon$ 12 – 16, $\Delta n \sim 0.075$, T_{NI} 70 – 85 °C	Very wide viewing angle and superior picture quality; nitrile based materials can also be used
VA-TFT	PC monitors	$\Delta\varepsilon \sim -4.5$, $\Delta n \sim 0.08$, $T_{NI} \sim 70$ °C	Very wide viewing angle and superior picture quality; very high contrast and fast switching time
Plasma Addressed LCD (PALC)	TV, advertising	$\Delta\varepsilon < 0$, $\Delta n \sim 0.08$, $T_{NI} \sim 70$ °C	Large size (1 m diagonal); very good picture quality and fast switching time

[a] The IPS mode is not based on a twisted nematic (TN) cell but on an interdigital electrode arrangement.[30]

utilization of their otherwise quite advantageous properties, such as low viscosity or low birefringence. Even for materials with a stable nematic phase, the comparative evaluation of their application potential is severely complicated by the strong dependence of all anisotropic parameters on the temperature and on the nematic–isotropic transition point of each individual compound.[8]

One method to obtain a set of comparable characteristics for any kind of material, independent of its phase sequence, is the introduction of so-called "virtual" parameters: nematic–isotropic transition points ($T_{NI,extr}$), electrooptic ($\Delta\varepsilon$, Δn), and viscoelastic parameters (γ_1) are measured in a defined solution of the respective single compound in a standardized nematic host mixture. The values thus obtained are empirically corrected for the change in the order parameter induced by the addition of the single compound and extrapolated to 100% pure, single compound. Even if, from the theoretical point of view, this method is based on some simplifying assumptions, in most cases the "virtual" parameters are linearly additive to a degree, sufficient for the calculation and prediction of mixture properties from these standardized single-compound properties. The practical development of commercial liquid crystal mixtures is based strongly on this method.

3. Material Requirements for Active Matrix Displays

In addition to the above-mentioned physicochemical requirements, liquid crystals for display applications also have to meet a different set of specifications, which are usually collected under the term "reliability". The exact definition of "reliability" varies for each application and also for each display manufacturer but every liquid crystal mixture, prior to commercialization, usually has to pass tests focusing on the purity, long term chemical and photochemical stability, and specific dielectric properties.

In desktop computer monitors, most components of the display are permanently heated by the backlight to sometimes more than 60 °C. Here, the long term stability of the liquid crystal mixture against thermal or photochemical degradation is a decisive point for the material development. Whole classes of materials with otherwise excellent properties, such as tolane (diphenylethyne) or (*E*)-stilbene ((*E*)-diphenylethene) -based liquid crystals, are generally not used for AM-LCDs due to their limited photochemical stability. High stability towards UV irradiation is especially important for materials used in projection displays with high pressure xenon or mercury lamps as the light source.

In an AM-LCD, the driving voltage is applied to each pixel once per refresh cycle. Until the next cycle, the voltage has to be kept constant by the capacitance of the liquid crystal layer and by the voltage-holding capacitor integrated into each pixel (Figure 2).

If there is a voltage drop, such as one due to an electric current leaking through the liquid crystal, the contrast of the display is reduced or flicker phenomena are observed.[44, 45] Reliability tests include measurements of the voltage-holding ratio (VHR, the ratio of the voltages applied to a pixel at the end and beginning of a defined timespan), the specific resistivity (SR),[46] and the ion density.[47] Additional reliability problems, such as image sticking, are caused by the residual direct current (DC),[48] which is linked to an inhomogeneous distribution of charge carriers within the liquid crystal cell after application of a voltage for a prolonged period.[49, 50] Changes in the ion density, VHR, SR, or of the clearing point under the influence of elevated temperatures or UV irradiation usually indicates chemical degradation of the liquid crystal or of another peripheral material, such as the alignment layer.

Insufficient reliability of a liquid crystalline material, especially an insufficiently low VHR, strongly affects the observable picture quality—and thereby also the production yield—of a display panel. Therefore, reliability has become one of the most decisive factors for the development of new materials designed for active matrix displays.

Already during the initial development phase of the AM-LCD technology, a body of evidence developed that indicated the cyano-based materials shown in Scheme 1 could not meet the stringent requirements on the specific resistivity and the VHR for active matrix displays. Even after extensive purification and removal of potential ionic contaminants, the VHR of most of these materials could not be raised to a sufficient level.[51]

Since the early 1980s, a large number of liquid crystals carrying fluorine substituents were synthesized. The initial interest in such materials was aroused by the greater nematic phase range, often dramatically increased, of laterally fluorinated liquid crystals compared to their nonfluorinated analogues. Later, it was found that liquid crystals that derive their molecular dipole moment not from a terminal cyano group but from one or more carbon–fluorine bonds—the so-called superfluorinated materials (SFMs)[52–54]—fulfilled the reliability requirements for materials used in AM-LCD.

4. Chemistry of Highly Fluorinated Liquid Crystals

Due to the high fluorination degree of most liquid cystals used in active matrix applications, a specialized methodology for the synthesis of these materials was developed. Usually the syntheses commence from aromatic building blocks already carrying the required fluorination pattern. These building blocks are either functionalized via their commercially available halogen derivatives or directly by *ortho*-metallation.[55] In 1989, when the first liquid crystals with an *ortho*-metallation step in their synthetic sequence were introduced to the market, it was also the first time that the necessary low temperature reactions ran on an industrial scale. The activated intermediates can be subsequently treated with a variety of organometallic C–C coupling reactions[56–58] to carbonyl compounds, (cyclo)alkyl bromides,[59] aromatic halides,[60] or boronic acids.[61] Other, often used, types of C–C coupling reactions are the Wittig reaction[62] and the Heck coupling (Scheme 2).[63]

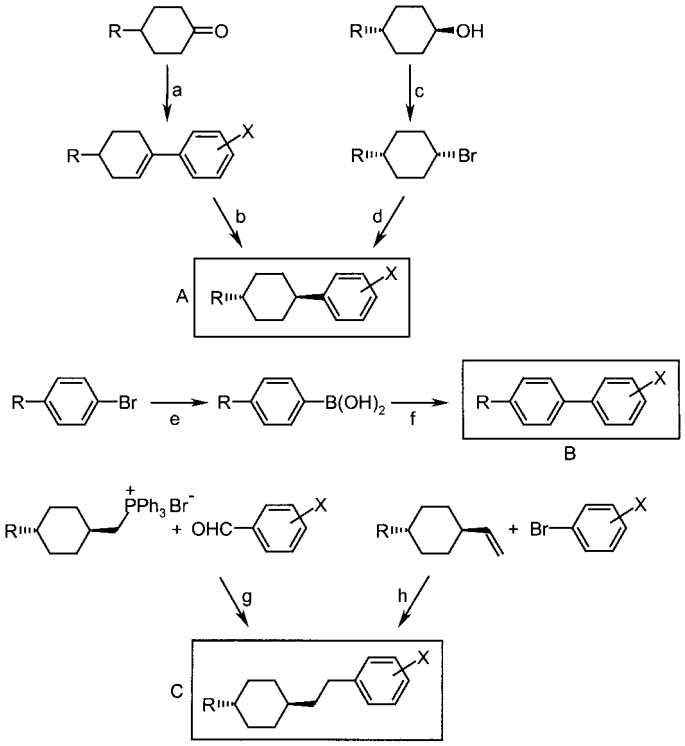

Scheme 2. General synthetic procedures with typical reaction conditions and yields for the important substructures of nematic liquid crystals: a) 1. ArMgBr, THF; RT, 2 h; 2. Cat. TsOH, toluene; azeotropic removal of water (50–60%). b) H_2, THF, 5% Pd/C (25–30% pure *trans* product). c) Ph_3PBr_2, CH_3CN; 0→50 °C, 5 h (80–85%). d) 1. Li, $ZnBr_2$, THF, toluene; sonication at 5–15 °C; 2. ArBr, 0.05 equiv $[Pd(dppf)Cl_2]$; RT, 48 h (50–60% pure *trans* product). e) 1. *n*BuLi, THF; −78 °C, 30 min; 2. $B(OMe)_3$; −78 °C→RT; 3. 2N HCl (75–80%). f) ArBr, aq. Na_2CO_3, toluene, 0.05 equiv $[Pd(PPh_3)_4]$; 50 °C, 18 h (70–80%). g) 1. KO*t*Bu, THF; −10 °C→RT; 2. H_2, 5% Pd/C, THF (80–90%). h) 1. ArBr, 0.05 equiv (*o*-tolyl)$_3$P, NEt_3, CH_3CN; reflux, 96 h; 2. H_2, 5% Pd/C, THF (85–90%). RT = room temperature, Ts = 4-toluene sulfonyl, dppf = 1,1′-bis(diphenylphosphinyl)ferrocene.

4.1. Materials for Standard AMD Applications

Currently, most AM-LCD in use as, for example, desktop computer monitors are based on 5 or 4 V driver circuits, that require a threshold voltage V_{th} of around 2 V for the liquid crystal mixture. The mixtures used for this applications usually have a dielectric anisotropy $\Delta\varepsilon$ value between four and six and a birefringence Δn in the range of 0.085 to 0.10, depending on the cell gap of the display and the choice of compensation films for the improvement of brightness or viewing angle independence of the contrast.

Cyano materials such as **1**, **2**, or **3** are not used due to their low voltage-holding ratio. Therefore, the required $\Delta\varepsilon$ value has to be achieved by other means, such as the dipole moment of terminal carbon–halogen bonds. The electronegativity differences ΔEN are 0.33 and 1.60 for the carbon–chlorine and the carbon–fluorine bond, respectively, while the lengths of the aromatic carbon–halogen bonds are 170 and 136 pm for chlorine and fluorine, respectively. A phenylcyclohexane-based liquid crystal with one terminal C_{ar}–F dipole[64] has a $\Delta\varepsilon$ value of only around four. One often applied method to increase the dielectric anisotropy is the introduction of additional lateral fluorine atoms in order to augment the molecular dipole moment.[52] As the comparison between **2**, **6**, and **7** illustrates (Table 2), it is generally much more difficult to achieve a high dielectric anisotropy with materials in which their polarity is based solely on carbon–halogen bonds than for cyano-based materials.

Table 2. Examples for the first generation of commercially used materials used in TN and AM-LCDs.[65]

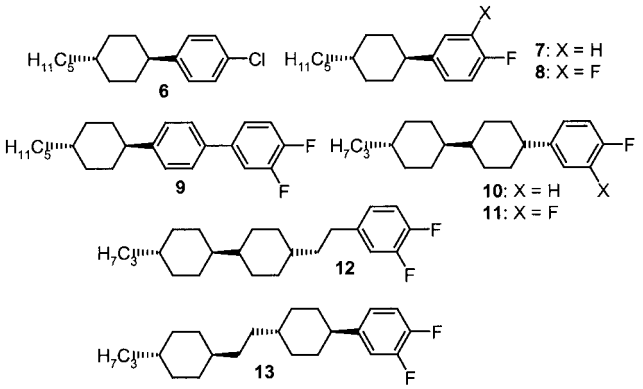

No.	Mesophases	$T_{NI,extr}$	$\Delta\varepsilon$	Δn	γ_1
1	C 23 N 35.1 I	4.2	21.6	0.237	112
2	C 31 N 54.6 I	25.7	18.0	0.125	199
3	C 56 N 72 I	49.8	16.8	0.128	–
4	C 65 S_B (52) N 86.2 I	34.3	8.3	0.067	408
5	C 34 N (19) I	14.1	−8.2[a]	0.027	–
6	C 32 I	−12.4	4.2	0.108	62
7	C 34 I	−56.9	4.0	0.075	27
8	C −6.1 I[b]	–	–	–	–
9	C 55 N 105.4 I	107.8	6.3	0.144	210
10	C 90 N 158.3 I	161.3	3.0	0.079	156
11	C 46 N 124.3 I	116.0	6.4	0.079	160
12	C 25 S_B 53 N 119.1 I	111.7	5.1	0.082	229
13	C 39 N 104.3 I	105.7	5.5	0.067	247

[a] Extrapolated from the Merck mixture ZLI-2857. [b] Data cited from ref. [52].

From the data shown in Table 2, a principal disadvantage of the superfluorinated materials (SFMs) becomes obvious immediately: The clearing points (real nematic–isotropic transitions as well as "virtual" extrapolated values) are much lower than for the cyano materials (**2**→**6**→**7**). On the other hand, the rotational viscosities γ_1 are also far lower, so that especially the fluorinated two-ring materials (**7**, **8**) become interesting as mixture components in order to reduce the switching time of the display. Comparison of the pair **10** and **11**, for example, shows that the lateral fluorination is effective for increasing the value of $\Delta\varepsilon$ by three to four units. On the other hand, the major drawback of the lateral fluorination strategy is a significant decrease of the clearing temperatures by 30 to 40 K for each lateral fluorine substituent.

In order to increase $\Delta\varepsilon$ values and avoid the concomittant decrease of the clearing points, the next logical step was to make use of the cumulated carbon–fluorine dipole moments of highly fluorinated terminal alkyl groups.[66]

As shown in Table 3, terminal perfluoroalkyl chains are well suited to achieve a strong dielectric anisotropy compared to the terminally fluorinated materials. On the other hand, use

Table 3. Examples for liquid crystals deriving their polarity from highly fluorinated terminal alkyl chains.[65]

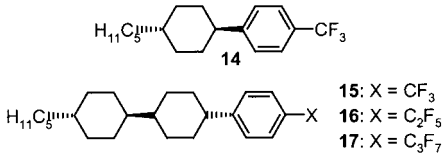

No.	Mesophases	$T_{NI,extr}$	$\Delta\varepsilon$	Δn
14	C 23 I	− 71.0	9.2	0.086
15	C 43 $S_?$ 109 N 122.9 I	100.0	9.1[a]	0.103[a]
16	C 89 N (88.6) I	116.1	6.3[a]	0.083[a]
17	C 127 N (126) I	110.8	7.5	0.084

[a] Extrapolated from the Merck mixture ZLI-1132.

of longer fluorinated side chains does not increase $\Delta\varepsilon$ but often results in higher melting temperatures and occasionally also in solubility problems. Despite their reasonably high virtual clearing temperatures, many of the highly fluorinated materials (such as **15**, **16**, or **17**) show only a monotropic nematic phase.

The synthesis of the (per)fluoroalkyl-substituted liquid crystals is based on the bromoaromatic building blocks of the type **20** (Scheme 3). They are attached to the basic mesogenic core structures by the general methods depicted in Scheme 2.[67]

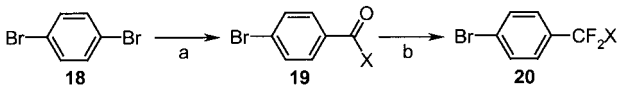

Scheme 3. Syntheses for highly fluorinated 4-alkyl-bromobenzenes (**20**), used as starting materials for the liquid crystals shown in Table 3: a) 1. *n*BuLi, THF; − 78 °C, 30 min; 2. EtOOC-R_f (R_f = CF_3, C_2F_5); − 78 °C, 2 h (70 – 85 %). b) Diethylaminosulfurtrifluoride (DAST), neat; 0 → 50 °C (**Caution:** sometimes decomposes explosively), 5 h (65 – 75 %).

As an alternative concept, which makes use of the advantages of highly fluorinated alkyl chains (namely, their strong dipole moment) while improving the mesogenic properties, fluorinated alkoxy functions were introduced to the basic mesogenic core structures (see Table 4).[68, 69]

In spite of their tendency to form smectic mesophases in the pure state, some of the materials based on a terminal trifluoromethoxy group (such as **23**) are playing a central role in commercially used standard AMD liquid crystal mixtures, together with the 3,4-difluorobenzene-derived materials (**11** – **13**; Table 2).[28] Compared to their structurally analogous 3,4-difluorobenzene derivatives, materials with a terminal trifluoromethoxy group possess higher clearing temperatures, which allows the operating temperature range for LCDs to be extended to higher temperatures.

Table 4. Liquid crystals with fluorinated alkoxy groups.[65]

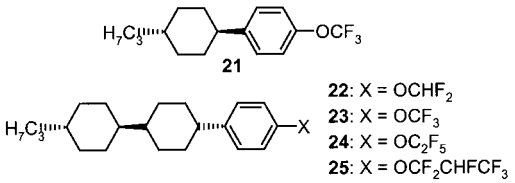

No.	Mesophases	$T_{NI,extr}$	$\Delta\varepsilon$	Δn	γ_1
21	C − 3 I	− 68.0	7.1	0.083	25
22	C 52 S_B 69 N 173.6 I	163.2	5.2	0.086	–
23	C 39 S_B 70 N 154.7 I	146.2	6.9	0.087	142
24	C 119 S_B 152 N 168.6 I	152.1	6.5	0.088	–
25	C 178 I	157.3	3.9	0.074	–

The synthesis of the building blocks (Scheme 4) used for this type of materials starts from 4-bromophenol **26** and involves three different types of reactions: Simple nucleophilic substitution (→**27**; probably via a difluorocarbene intermediate),[70] nucleophilic substitution followed by a Lewis acid catalyzed fluorination (→**28**; Swarts-type reaction),[71] nucleophilic addition to perfluoroolefins (→**29**),[72] or fluorination of an intermediate trifluoroacetate (→**30**) with sulfur tetrafluoride to the pentafluoroethoxy function (→**31**).[73]

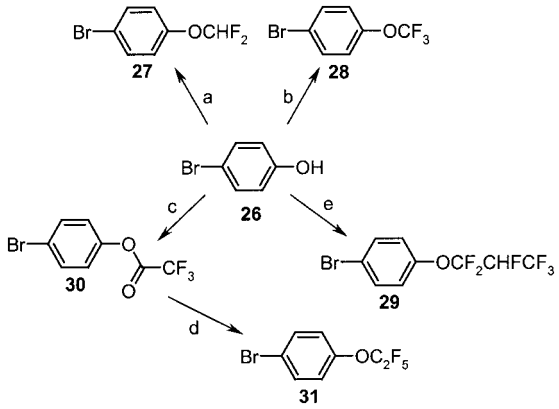

Scheme 4. Syntheses for highly fluorinated 4-alkoxy-bromobenzenes used as starting materials for the liquid crystals shown in Table 4: a) KOH, $CHClF_2$, dioxane/H_2O (1/1); 40 °C, 1 – 3 bar, 4 h (55 %). b) CCl_4, HF; 150 °C, 18 h (61 %). c) $(CF_3CO)_2O$ neat; reflux, 5 h. d) SF_4, HF; 100 → 175 °C over 10 h (70 – 75 %). e) NEt_3, $F_2C{=}CFCF_3$; 75 °C, 45 min (53 %).

The main characteristic of the materials listed in Tables 2 – 4 is their strong dielectric anisotropy $\Delta\varepsilon$. This basic property is sometimes accompanied by relatively low clearing temperatures T_{NI}, high rotational viscosities γ_1, or a narrow nematic phase range. In order to improve the operating temperature range of the display and to adjust the birefringence Δn and dielectric anisotropy to the exact specifications dictated by the display design, often less polar compounds are used to fine tune the liquid crystal mixture.[28] Some commonly used examples of such materials are listed in Table 5.

Compounds **35** and **36** have an olefinic side chain. Such materials often have lower rotational viscosities γ_1 and a more pronounced tendency to form a nematic mesophase than their saturated analogues.[74, 75] The synthetic strategy leading to alkenyl compounds, such as **36**, is based on Wittig reactions, either for the homologation of carbonyl compounds by one to two carbon atoms or for the generation of the double bonds in the side chain (Scheme 5).[76]

The comparison between the four-ring materials **37**[77] and **38**[78] demonstrates the aforementioned expansion of the nematic phase range upon lateral fluorination.[79]

Table 5. "Neutral" materials used for miscellaneous purposes, such as the exact adjustment of electrooptic properties, reduction of the rotational viscosity, or increasing the clearing temperature of mixtures for LCDs.[65]

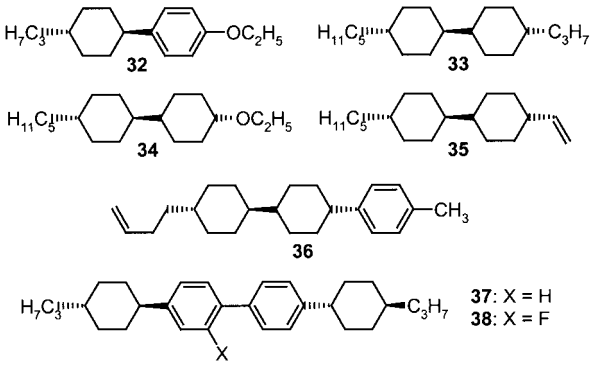

No.	Mesophases	$T_{NI,extr}$	$\Delta\varepsilon$	Δn	γ_1
32	C 42 N (37.6) I	28.3	– 0.1	0.098	44
33	C 22 S_B 98 I	56.2	– 0.5	0.049	31
34	C 49 N 49.6	27.2	– 0.4	0.048	46
35	C – 9 S_B 52 N 63.1 I	51.8	0.3	0.054	39
36	C 54 S_B 104 N 176.6 I	186.5	– 1.0	0.097	159
37	C 158 S_B 212 S_A 223 N 327	330	– 0.1	0.137	491
38	C 133 N 302 I	299.5	0.0	0.126	651

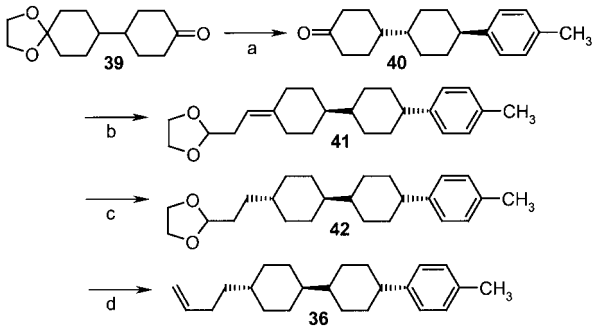

Scheme 5. Example synthesis of the alkenyl compound **36**: a) 1. 4-MePhMgBr, THF; 2. cat. TsOH, toluene; azeotropic removal of water (70%); 3. H_2, 5% Pd/C, THF; 4. 98% HCOOH, toluene; 5. selective crystallization of the *trans* isomer from *n*-heptane (40–60%). b) 2-(1,3-dioxolan-2-yl)ethylphosphonium bromide, KO*t*Bu, THF; –10 °C→RT. c) H_2, 5% Pd/C, THF (64%). d) 1. 98% HCOOH, toluene; 2. $MePPh_3^+Br^-$, KO*t*Bu, THF; –10 °C→RT (66%).

4.2. Materials for Displays with Low Driving Voltages

Recently, on the side of LCD manufacturers there is a trend to reduce the driving voltage, especially for notebook computer displays. A reduction of the driving voltage from 4–5 V to 3.3 V or even 2.5 V allows a denser integration of the electronic components, which is, of course, an advantage for portable devices. The power consumption of the electronic components of the display is also lower, to result in a longer battery lifetime. For the liquid crystal material, a reduced driving voltage requires a lower threshold voltage V_{th} for the electrooptical response, which is most effectively met by increasing the dielectric anisotropy $\Delta\varepsilon$.

The consequent application of this lateral fluorination concept in order to increase $\Delta\varepsilon$ leads from the 3,4-difluorobenzene derivatives (Table 2) to the 3,4,5-trifluorobenzene-based liquid crystals listed in Table 6.[68, 80]

Table 6. Materials deriving their polarity from a 3,4,5-trifluorophenyl group.[65][a]

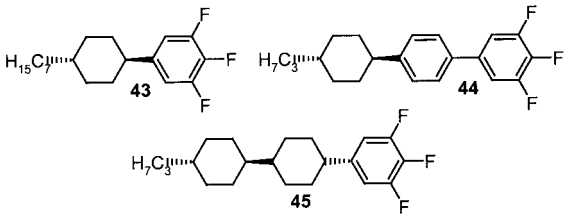

No.	Mesophases	$T_{NI,extr}$	$\Delta\varepsilon$	Δn	γ_1
43	C 25.6 I	– 103.0	6.8	0.034	49
44	C 40.7 N (33.2) I	57.8	12.8	0.137	151
45	C 64.7 N 93.7 I	74.0	8.3	0.073	171

[a] Except γ_1 values, all data are cited from ref. [80].

The values of the dielectric anisotropies $\Delta\varepsilon$ of this class of substance range between 7 and 13, depending on the mesogenic core structure. The rotational viscosities γ_1 are also reasonably low, allowing for displays with switching times compatible with video demands. Nevertheless, the lateral difluorination results in a severe drop of real as well as of virtual clearing temperatures of the two and three-ring materials. In order to address this problem, the lateral fluorination concept was combined with polar terminal groups, such as trifluoromethoxy and difluoromethoxy moieties, which are known to induce higher clearing temperatures.[53, 54]

In the first generation of liquid crystal mixtures for use in AM-LCD at low driving voltages, compound **47** and its alkyl homologues played an especially dominant role. While the laterally nonfluorinated materials in Table 4 have a tendency to form smectic phases, the laterally fluorinated liquid crystals in Table 7 are all purely nematic.

The syntheses of laterally fluorinated (per)fluoroalkoxy compounds are based on *ortho*-metallation[55, 81] of precursors such as **52**.[13] The lithiated species is oxidized to the phenol via a boronic ester intermediate and, subsequently, converted to the desired liquid crystals by the general methods shown in

Table 7. Materials with increased dielectric anisotropy by lateral fluorination or difluorination.[65]

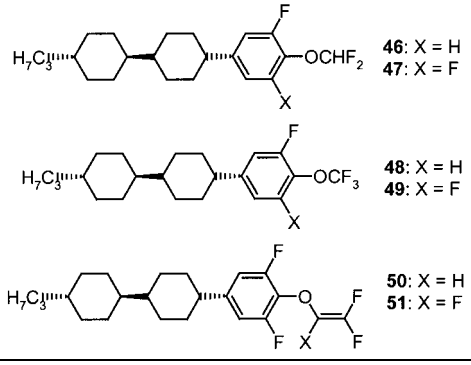

No.	Mesophases	$T_{NI,extr}$	$\Delta\varepsilon$	Δn	γ_1
46	C 33 N 144.6 I	123.8	7.4	0.087	242
47	C 62 N 127.5 I	86.9	8.8	0.083	313
48	C 46 N 129.8 I	107.9	9.0	0.089	200
49	C 66 N 118.3 I	86.2	10.5	0.083	279
50	C 49 N 135.9 I	105.3	9.8	0.099	132
51	C 64 N 80.9 I	53.6	10.7	0.088	158

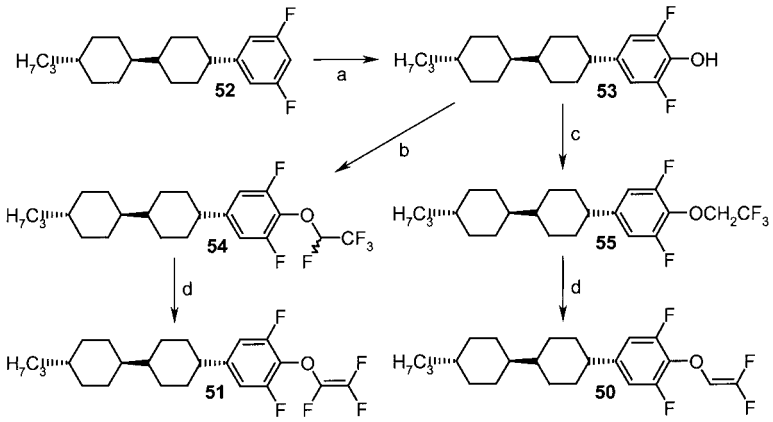

Scheme 6. Syntheses for liquid crystals **50** and **51**: a) 1. *n*BuLi, THF; −70 °C, 30 min. 2. $B(OMe)_3$; −70 °C→RT. 3. 30 % H_2O_2, HOAc; 30→50 °C (50–60 %). b) 1. CF_3CHO, THF; 5 °C, 30 min; 2. DAST, CH_2Cl_2; 10 °C→RT, 18 h (35 %). c) 1. NaH, THF; 2. $TsOCH_2CF_3$; reflux, 18 h (45 %). d) LDA, THF; −70 °C→RT (70–90 %). LDA = lithium diisopropylamide.

Scheme 2. The fluoroalkenyloxy derivatives **50** and **51** are synthesized as depicted in Scheme 6.[82, 83]

If the lateral fluorination concept is applied to additional aromatic rings in the mesogenic core structure, materials with dielectric anisotropies $\Delta\varepsilon$ up to about 20 (**57** in Table 8) can be obtained.[84] On the other hand, the same example also illustrates the extreme effect multiple lateral fluorination has on the (virtual) clearing temperature, which has dropped below 0 °C.

Table 8. Materials with increased dielectric anisotropy by lateral fluorination or difluorination on a second ring structure.[65]

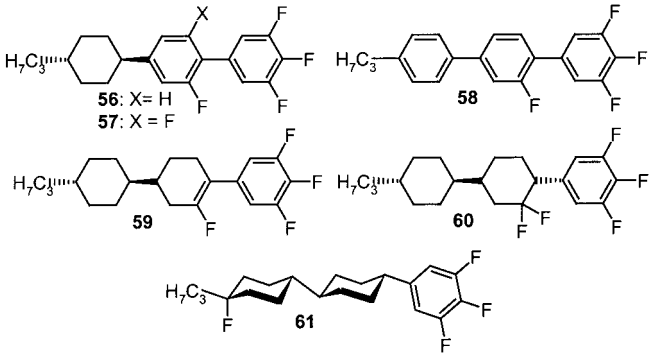

No.	Mesophases	$T_{NI,extr}$	$\Delta\varepsilon$	Δn	γ_1
56	C 64 I	25.0	15.2	0.135	173
57	C 123 I	−9.6	20.5	0.117	–
58	C 54 N (35.7) I	39.7	17.6	0.219	168
59	C 46 N 69.6 I	60.8	15.1	0.093	210
60	C 65 I	25.8	13.9	0.075	508
61	C 73 N 115 I	89.4	9.8	0.082	301

Materials such as **56**, **57**, or **58** are usually synthesized by repetitive *ortho*-metallation, iodination, and subsequent palladium-catalyzed addition of the ring increments as boronic acids (Scheme 7).

The introduction of a second aromatic substructure in order to attach the additional lateral fluorine atoms leads to a concomittant increase in birefringence (for example **45**→**44**). If a lower birefringence is required, it is possible to (on paper)

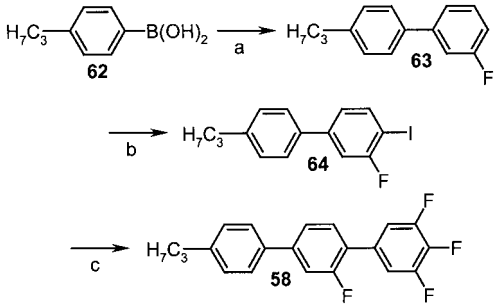

Scheme 7. Example of the sequential synthesis of a terphenyl-based liquid crystal (**58**): a) 3-Fluorobromobenzene, Na_2CO_3, EtOH, toluene, 0.03 equiv $[Pd(PPh_3)_4]$; 50 °C, 18 h (92 %). b) 1. KO*t*Bu, BuLi, THF; −100 °C; 2. I_2; −100 °C→RT (51 %). c) 3,4,5-Trifluorophenylboronic acid, 0.03 equiv $[Pd(PPh_3)_4]$, Na_2CO_3, EtOH, toluene; 50 °C, 18 h (98 %).

"reduce" the second aromatic moiety to a cyclohexene structure (**59**), which can also serve as a scaffold to attach the fluorine atom but does not contribute so much to the anisotropy of the molecular polarizability (Scheme 8).[85]

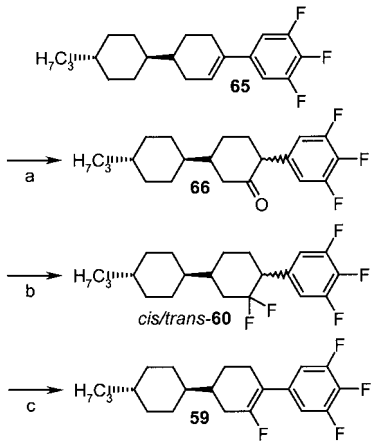

Scheme 8. Synthesis of the fluorocyclohexene-based liquid crystal **59**: a) 1. $BH_3 \cdot THF$; 2 °C→RT; 2. 30 % H_2O_2, HOAc; RT→35 °C (66 % isomer mixture); 3. PCC, CH_2Cl_2; RT, 18 h (85–90 %). b) DAST, CH_2Cl_2; reflux (86 % crude product). c) KO*t*Bu, THF; 70 °C, 5 h (76 %). PCC = pyridiniumchlorochromate.

A recent approach to compensate the unacceptably low clearing temperatures of highly fluorinated liquid crystals is the exchange of axial hydrogen atoms of cyclohexane substructures by fluorine. Materials such as **61** ($T_{NI} = 115$ °C) generally have virtual clearing points 10–15 K higher than their axially nonfluorinated analogues (**45**: $T_{NI} = 93.7$ °C).[86, 87]

The reduction of the threshold voltage V_{th} of a liquid crystal mixture by exclusively increasing the dielectric anisotropy also increases the average dielectric constant ($\varepsilon_{mean} = (\varepsilon_{\parallel} + 2\varepsilon_{\perp})/3$). Materials with a high ε_{mean} value promote the dissociation of ionic trace impurities, to result in a decrease in the VHR and specific resistivity.[44, 80] Therefore, a more differentiated approach is the utilization of mixture components with a small elastic constant K_1 for the "splay" deformation, according to Equation (2).[53] A substance class generally suitable for this strategy are fluorinated phenol

esters, such as **67**–**70** (Table 9). Even if an ester-based mixture has a lower overall dielectric anisotropy, it can still have a lower threshold voltage for the electrooptical response than a conventional ester-free material.

Table 9. Strongly polar, phenol ester structures.[65]

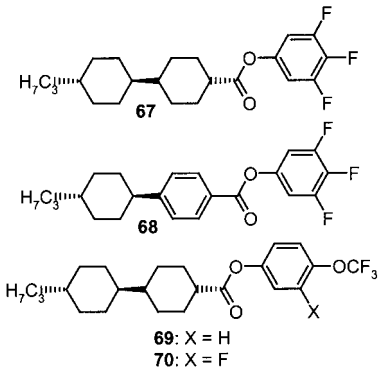

No.	Mesophases	$T_{NI,extr}$	$\Delta\varepsilon$	Δn	γ_1
67	C 56 N 117.2 I	110.6	11.1	0.067	175
68	C 101 N (90) I	82.8	21.4	0.129	216
69	C 52 S_B 126 N 187.4 I	172.3	6.2	0.078	199
70	C 50 N 159.3 I	142.1	8.9	0.071	235

Of course, the ester structure is potentially always sensitive towards hydrolysis, thus limiting the chemical stability of the liquid crystal material. For this reason, the more inert difluorooxymethylene bridge was intensively investigated as an alternative, inherently polar linking group for liquid crystals (Table 10).[88]

Table 10. Structures deriving additional polarity from a polar difluorooxymethylene link within the mesogenic core.[65]

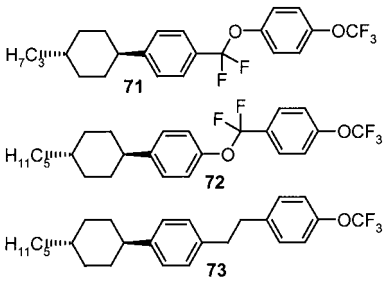

No.	Mesophases	$T_{NI,extr}$	$\Delta\varepsilon$	Δn	γ_1
71	C 57 S_B 70 N 82.9 I	69.7	9.1	0.115	93
72	C 43 S_B 116 I	100.2	4.4	0.105	–
73	C 47 S_B 68 N 73.7 I	62.3	6.5	0.120	204

Use of this group, as exemplified by **71**, results in a significant increase of $\Delta\varepsilon$ compared to the ethylene-linked reference compound **73**, since the dipole moments of the polar terminal trifluoromethoxy group and of the polar difluorooxymethylene bridge are added. If the direction of the linking group is reversed, the dielectric anisotropy is decreased (**72**).

Difluorooxymethylene-based liquid crystals can be synthesized from 4-bromobenzaldehyde **74**, which is fluorinated with diethylaminosulfurtrifluoride (DAST), photobrominated, and treated with the corresponding phenolate (Scheme 9). The resulting intermediate **77** is coupled to the zinc derivative of a suitable *cis*-4-alkylbromocyclohexane.[89]

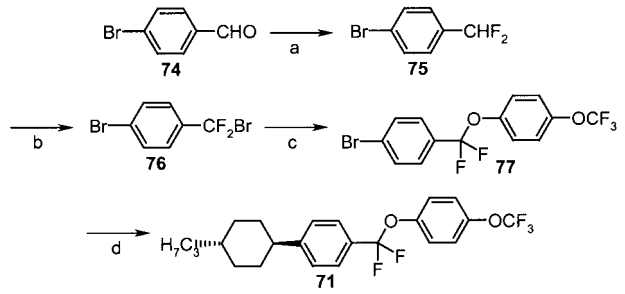

Scheme 9. Synthesis of the difluoroxymethylene-linked liquid crystal **71**: a) DAST, CH_2Cl_2; reflux, 18 h (80%). b) Br_2, CCl_4; *hv*, 14 d (70–80%). c) 3,4,5-trifluorophenol, NaH, DMF; 50–60 °C, 15 h (51%). d) 1. *cis*-4-propylbromocyclohexane, Li, $ZnBr_2$, THF, toluene; sonication, RT, 4 h; 2. **77**, cat. [Pd(dppf)Cl_2], THF, toluene; RT, 18 h (46%).

An alternative method to augment the dipole moment of a polar terminal group is the introduction of a polar ring increment into the mesogenic core structure.[90, 91] Replacement of a cyclohexane substructure by a 1,3-dioxane unit leads to a dramatic increase in the value of $\Delta\varepsilon$ without the pronounced drop of the clearing temperatures, which is observed for lateral fluorination (Table 11). The dioxane-based materials **78**–**80** are synthesized by acid catalyzed reaction of an aldehyde with a suitable 1,3-diol.[90]

Table 11. Structures that derive additional polarity from a polar 1,3-dioxane subunit within the mesogenic core.[57]

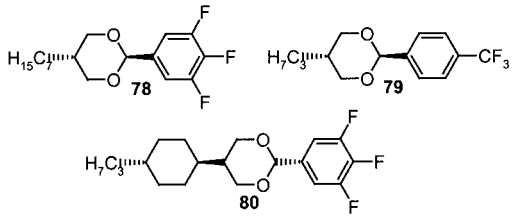

No.	Mesophases	$T_{NI,extr}$	$\Delta\varepsilon$	Δn	γ_1
78	C 20 I	– 97.6	15.2	0.080	–
79	C 57 I	– 88.3	16.1	0.093	–
80	C 74 N (51.2) I	69.7	17.0	0.068	201

The most severe drawback of liquid crystals carrying lateral fluorine atoms at aromatic substructures still are their low clearing temperatures compared to, for example, the cyano derivatives. Therefore, it is a most important target for application-oriented liquid crystal research to identify new, highly polar terminal groups, which induce reasonably high clearing points and have a minimized interaction with ionic trace impurities. The most polar liquid crystals resulting so far from this line of research are based on sulfur in its highest oxidation state (Table 12).[82, 92]

A terminal pentafluorosulfuranyl group[92] has a chemical stability comparable to the trifluoromethyl group. The resulting materials are more polar than the corresponding trifluoromethyl analogues.[93] Judging from its influence on the

Table 12. Highly polar liquid crystals based on sulfur-containing terminal groups.[65]

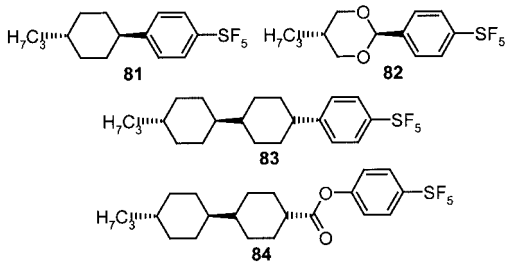

No.	Mesophases	$T_{NI,extr}$	$\Delta\varepsilon$	Δn	γ_1
81	C 11 I	– 96.8	12.0	0.087	133
82	C 69 I	– 79.9	20.2	0.091	145
83	C 121 I	97.8	11.6	0.094	612
84	C 90 N 152.8 I	132.9	12.3	0.087	–

electrooptic properties of liquid crystals, the pentafluorosulfuranyl group can be considered as a kind of "supertrifluoromethyl" group. The central building block **85**, which carries the pentafluorosulfuranyl function, is most conveniently prepared by direct fluorination of the disulfide **86**,[94] followed by hydrogenation and the Sandmeyer reaction. The bromide **85** can be converted to other building blocks, such as **88** or **89**, via its lithiated derivative (Scheme 10).

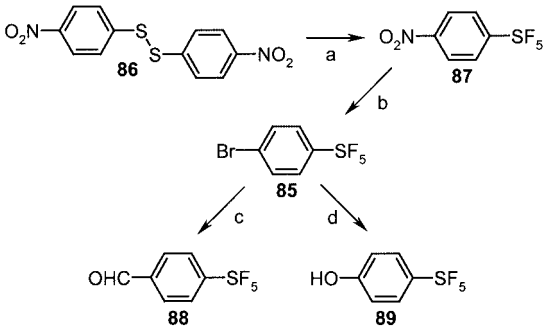

Scheme 10. Synthesis of the central building blocks **85**, **88**, and **89** for pentafluorosulfuranyl-based liquid crystals: a) 10% F_2 in N_2, CH_3CN; $-10\,^{\circ}C$ (80%). b) 1. H_2, 5% Pd/C, THF; 2. HBr, $NaNO_2$; $-5\,^{\circ}C$; 3. CuBr; RT $\rightarrow 80\,^{\circ}C$ (46%). c) 1. *t*BuLi, Et_2O, $-78\,^{\circ}C$; 2. *N*-formylpiperidine; $-40\,^{\circ}C \rightarrow$ RT (76%). d) 1. *t*BuLi, Et_2O, $-78\,^{\circ}C$; 2. $B(OMe)_3$; $-70 \rightarrow -20\,^{\circ}C$; 3. 30% H_2O_2, HOAc; $-20 \rightarrow 35\,^{\circ}C$, 1 h (58%).

4.3. Materials with Very Low Birefringence

The largest contribution to the overall power consumption of a LCD (about 70–90%) is due to the backlight used to illuminate the display. Recently, many portable devices, such as small notebook computers, video games, or personal digital assistants (PDAs, such as electronic notebooks and calendars), have therefore been equipped with reflective TFT displays[95] in order to increase the battery lifetime. Since the optical path of the reflected light through a reflective display is different from a usual TN-LCD, there are other requirements for the birefringence of the liquid crystal materials. While a standard TFT display requires a Δn value of roughly around 0.1, an optimal picture quality reflective with TFT display materials need Δn values around 0.06.

One possible empirical approach to materials with very low birefringence is the minimization of the number of polarizable structure elements, such as double or triple bonds within the molecule. On the other hand, the indirect contribution of the polarizability to the molecular dipole moment via induced dipole components makes it relatively difficult to obtain a large dielectric anisotropy $\Delta\varepsilon$ with purely cycloaliphatic materials. This effect is illustrated by the trifluormethyl bicyclohexane **90**,[96] which has a significantly lower virtual $\Delta\varepsilon$ than its structurally similar phenylcyclohexane analogue **14**,[66] that carries the same polar terminal group (Table 13).

Table 13. Polar two-ring structures with very low birefringence based solely on alicyclic substructures in the mesogenic core.[65]

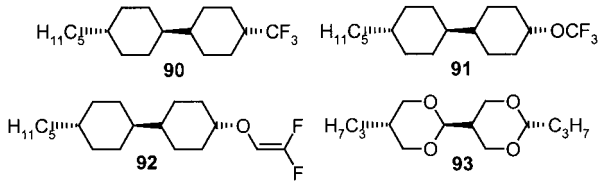

No.	Mesophases	$T_{NI,extr}$	$\Delta\varepsilon$	Δn	γ_1
90	C 35 S_3 (33) I	– 20.5	5.3	0.051	99
91	C 33 N (18.2) I	– 13.2	6.9	0.059	89
92	C 34 N (31.0) I	15.1	5.6	0.065	65
93	C 82 S_B 125 I	– 0.7	8.3	0.048	98

This difficulty was also addressed by combination of two 1,3-dioxanes within the mesogenic core structure (**93**).[97] Unfortunately, many of the more polar structures with low birefringence suffer from broad smectic mesophases or low solubility (**93**) in liquid crystal mixtures.

Due to the sensitivity of many cyclohexane-derived substances (such as **91**) towards base- or acid-catalyzed elimination, the introduction of the polar terminal groups must rely on a completely different methodology than for the aromatic derivatives. Thus, the trifluoromethyl function is most conveniently introduced by reaction of the corresponding *trans*-carboxylic acid with sulfur tetrafluoride (Scheme 11).[96, 98] The aliphatic trifluoromethoxy group is available by oxidative

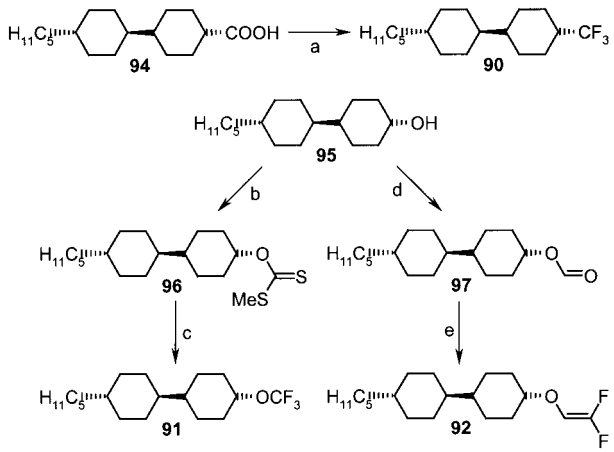

Scheme 11. Synthesis of the bicyclohexane derivatives **90**–**92**: a) SF_4, HF, CH_2Cl_2; 120 °C, 10 h (80%). b) 1. NaH, THF; 40 °C, 2 h; 2. CS_2; RT, 30 min; 3. MeI; RT, 18 h (93%). c) NBS, 50% HF/pyridine (20–30%). d) HCOOH, DCC, CH_2Cl_2; $0\,^{\circ}C \rightarrow$ RT (74%). e) $P(NMe_2)_3$, CF_2Br_2, THF/dioxane (10/1); $0\,^{\circ}C \rightarrow$ RT (42%). NBS = *N*-bromosuccinimide.

desulfurization of a methyl xanthogenate **96** in the presence of a fluoride ion source.[71c, 99] The difluorovinyloxy function is introduced by a modified Wittig-type reaction with a formate ester **97**.[97, 100]

The key step for the synthesis of the bis(1,3-dioxane) derivative **93** is the trimethylsilyltriflate-catalyzed ketalization[101] of the bis(trimethylsilyloxy) derivative **98** with butyraldehyde in order to avoid oligocondensation of the "ambivalent" (protected aldehyde and diol) intermediate **99** (Scheme 12).

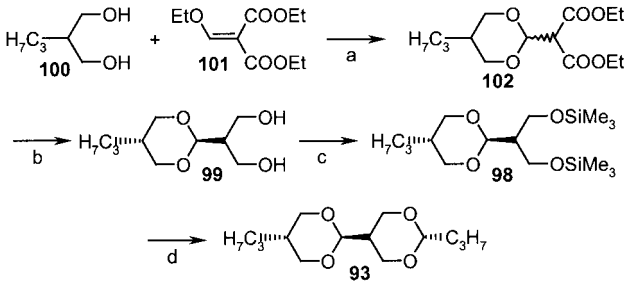

Scheme 12. Synthesis of the bis(1,3-dioxane) derivative **93**: a) Xylene, cat. TsOH; removal of EtOH by distillation (53%). b) 1. $LiAlH_4$, THF; 2. Isomer separation by crystallization from CH_3CN (29%). c) Me_3SiCl, NEt_3, DMF; 0 °C→RT (90%). d) H_7C_3CHO, cat. Me_3SiOTf, CH_2Cl_2; −78 °C, 30 min (21%). OTf = trifluormethane sulfonate.

Since the clearing points of the two-ring materials listed in Table 13 are relatively low with regard to display applications, some additional mixture components with low birefringence Δn, high clearing temperatures, and a broader nematic phase range are required.[102]

From the data in Tables 13 and 14, a common problem for the development of liquid crystal mixtures with very low birefringence becomes obvious: Nearly all materials with mesogenic core structures based only on cyclohexane have, in the best case, only very small nematic phase ranges. For this reason, in the future it will remain a very challenging task to develop mixtures for reflective TFT displays with a broad operating temperature range and low driving voltage.

Table 14. Materials with very low birefringence and high clearing points.[65]

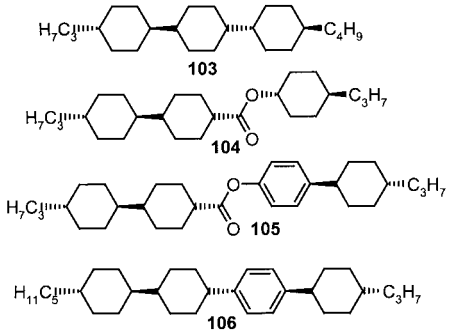

No.	Mesophases	$T_{NI,extr}$	$\Delta\varepsilon$	Δn
103	C 21 S_B 265 I	251.7	−0.1	0.057
104	C 59 S_B 154 N 190.2 I	196.9	−1.3	0.041
105	C 110 S_B 212 N 325 I	338.1	−0.6	0.072
106	C 36 S_B 313 N 322.5 I	315.1	−0.3	0.077

4.4. Dielectrically Negative Materials

Recently, AM-LCDs based on dielectrically negative liquid crystals were introduced to the market. These devices are mostly used for desktop computer monitors and, compared to standard AM-LCD, they offer a superior picture quality due to their high contrast ratio, wide viewing angle, and fast switching time.[28, 103]

In dielectrically negative materials, the dipole moment is ideally oriented perpendicular to the orientational axis ($\beta = 90°$).[38] In contrast to a "standard" TN cell with a positive $\Delta\varepsilon$ material, the dielectrically negative liquid crystals are oriented homeotropically (namely, perpendicularly) to the alignment layer in the cell. If a voltage is applied, the molecules experience a torque towards an orientation perpendicular to the applied electric field.

In principle, there are two different ways to attach a perpendicular dipole to a typical liquid crystal structure.[19] In materials containing a cyclohexane substructure, the axial hydrogen atoms—directed in an exactly perpendicular direction to the molecular long axis—can be replaced by polar moieties, such as cyano groups[18] (such as in **5**) or fluorine.[86, 104, 105] In aromatic substructures, the unilateral 2,3-positions can be substituted pairwise by fluorine, in a way that the dipole vector components in the direction of the long molecular axis cancel.

Materials of the latter type (Table 15)[106] are typical components of the dielectrically negative liquid crystal mixtures used, for example, in multidomain vertical alignment thin-film transistor (MVA-TFT) displays.[103]

Table 15. Examples for the first generation of dielectrically negative liquid crystals suitable for AM-LCD.[65]

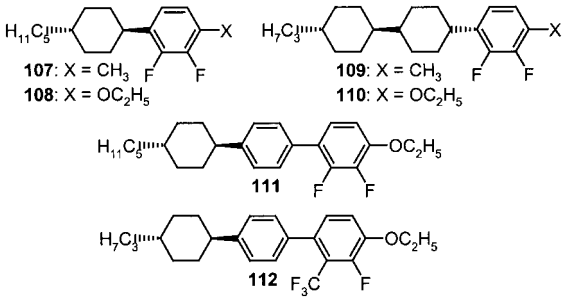

No.	Mesophases	$T_{NI,extr}$	$\Delta\varepsilon$[a]	Δn	γ_1
107	C 14 I	−49.2	−1.8	0.086	62
108	C 49 N (12.9) I	16.5	−6.2	0.099	110
109	C 67 N 145.3 I	139.0	−2.7	0.095	218
110	C 79 S_B (78) N 184.5 I	175.4	−5.9	0.096	413
111	C 74 S_A 86 N 170.7 I	190.6	−5.3	0.146	344
112	C 80 I	44	−7.3	0.133	637

[a] Extrapolated from the Merck mixture ZLI-2857.

The synthesis of this type of materials starts with 1,2-difluorobenzene **113**, which is derivatized in successive *ortho*-metallation steps (Scheme 13).[55]

The replacement of one fluorine atom by the more polar trifluoromethyl group[19] results in a further increase of the (negative) dielectric anisotropy but also in a severe drop of the virtual clearing temperature. This very pronounced effect

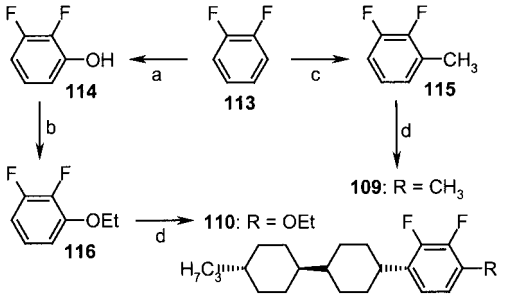

Scheme 13. Synthesis of the dielectrically negative materials **109** and **110**: a) 1. *n*BuLi, THF, −70 °C; 2. $B(OMe)_3$; −70 °C→RT; 3. 30 % H_2O_2, HOAc; RT→50 °C (90 %). b) EtBr, K_2CO_3, acetone; reflux, 18 h (94 %). c) 1. *n*BuLi, THF, −70 °C; 2. MeI; −70 °C→RT (77 %). d) 1. *n*BuLi, THF, −70 °C; 2. 4-propylbicyclohexan-4′-one; 3. Cat. TsOH, toluene; azeotropic removal of water; 4. H_2, 5 % Pd/C, THF (**109**: 35 %, **110**: 38 %).

is presumably due to a decrease of the length-to-breadth ratio of the molecule **112** compared to its analogue **111** (see Scheme 14 for synthesis).

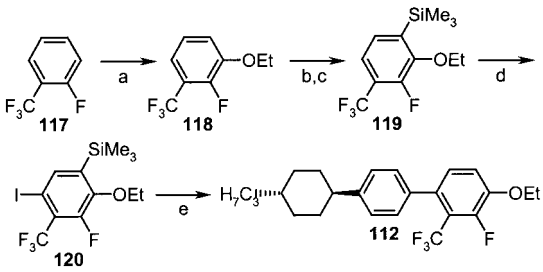

Scheme 14. Synthesis of the fluorotrifluoromethylbiphenylcyclohexane derivatives **112**: a) 1. *n*BuLi, THF; −70 °C; 2. $B(OMe)_3$; −70 °C→RT; 3. 30 % H_2O_2, HOAc; RT→50 °C; 4. EtBr, K_2CO_3, ethylmethylketone; reflux, 18 h (58 %). b) 1. *n*BuLi, THF; −70 °C; 2. I_2, THF; −70 °C→RT (76 %). c) 1. *n*BuLi, Et_2O; −70 °C; 2. Me_3SiCl, Et_2O; −70 °C→RT (70 %). d) 1. *n*BuLi, KO*t*Bu, THF; −78 °C; 2. I_2, THF; −78 °C→RT (59 %). e) 1. 4-Propylcyclohexylphenylboronic acid, 0.05 equiv $[Pd(PPh_3)_4]$, 2 N aq. Na_2CO_3, toluene; 50 °C, 18 h (60 %); 2. DMF, CsF; 80 °C, 1 h (quant.).

A less favourable property of the materials listed in Table 15 is their relatively high rotational viscosity γ_1, which limits the switching time. Therefore, as an alternative approach, liquid crystals based on axially fluorinated cyclohexane structures were extensively studied (Table 16).[86, 104]

The first objective, the reduction of γ_1, was clearly achieved. Further, as already mentioned before, the (virtual) clearing points are increased significantly compared to their axially nonfluorinated analogues—in the case of the bicyclohexane derivatives (such as **121**) by 50 to 70 K. Repetition of ethylene linked *ax*-fluorocyclohexane units (**121**→**123**→**125**) results in a further increase of the (negative) $\Delta\varepsilon$ values. With three repetitive units, the concept meets its limitations, since **125** is not sufficiently soluble in typical liquid crystal mixtures in order to measure properties for extrapolation.[65]

The doubly alkyl-substituted bicyclohexanes **121** have a strong tendency to form smectic B phases and, in higher concentrations, cause liquid crystal mixtures to become smectic on extended storage at low temperatures. Introduction of double bonds into the side chains suppresses the smectic phases and a nematic phase emerges, as demonstrated by **122** and **124**.[75, 105]

Table 16. Dielectrically negative liquid crystals based on axially fluorinated cyclohexane subunits.[65]

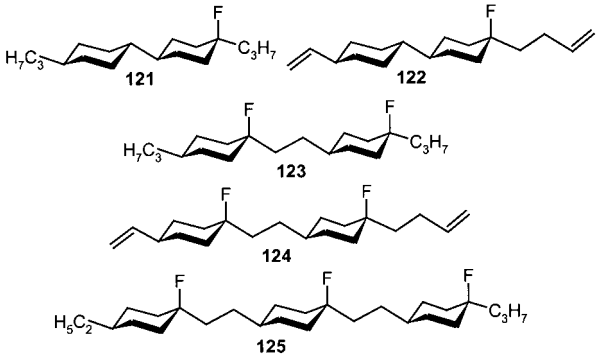

No.	Mesophases	$T_{NI,extr}$	$\Delta\varepsilon$[a]	Δn	γ_1
121	C 75 S_B 94 I	79.6	−2.2	0.054	–
122	C 13 S_B 37 N 79.8 I	56.5	−1.9	0.057	41
123	C 78 S_B 105 I	76.5	−4.6	0.051	198
124	C 74 S_B (70) N 83.0 I	37.3	−3.8	0.061	156
125[b]	C >120, dec.	–	–	–	–

[a] Extrapolated from the Merck mixture ZLI-2857. [b] Compound **125** could not be fully characterized due its insufficient solubility.

The synthesis of axially fluorinated cyclohexane derivatives is generally based on Wittig olefinations and a subsequent hydrofluorination step (Scheme 15). Surprisingly, the selectivity of 70 % HF/pyridine (Olah's reagent)[107] is so high, that even tetraenes such as **131** are smoothly and selectively converted into the difluorinated bis(alkenyl) compound **124**.

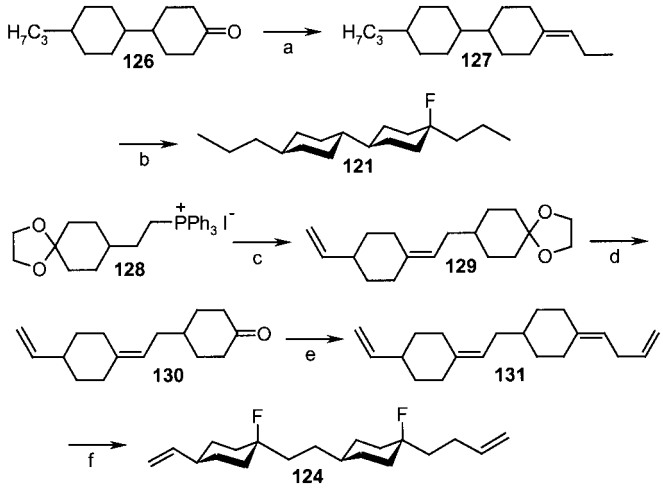

Scheme 15. Synthesis of the liquid crystals **121** and **124**: a) $H_7C_3PPh_3^+Br^-$, THF; −10 °C→RT, 2 h (80–90 %). b) 20 equiv 70 % HF/pyridine, CH_2Cl_2; RT, 18 h (35 %). c) 4-Vinylcyclohexanone, KO*t*Bu, THF; −10 °C→RT, 4 h (95 %). d) HCOOH, toluene; RT, 18 h (73 %). e) $H_2C{=}CHCH_2CH_2PPh_3^+Br^-$, THF; −10 °C→RT, 2 h (55 %). f) 1. 4 equiv 70 % HF/pyridine, CH_2Cl_2; −15 °C→10 °C, 1 h; 2. Recrystallized three times from *n*-pentane (6 %).

5. Tools for the Rational Design of Liquid Crystals

Much of the materials research in the liquid crystal field is characterized by empirical structure–property relationships. Some of those are straightforward, such as the increase in $\Delta\varepsilon$ upon the introduction of stronger polar terminal substituents or the lowering of Δn by minimizing the number of polarizable groups. Others are perhaps less obvious, such as the suppression of smectic phases by lateral fluorination or the enhancement of the nematic phase range after the replacement of fluorinated aromatics by heterocyclic analogues.[108] Other properties, such as rotational viscosities, elastic constants, or the nature and range of mesophases, are only related in an indistinct and unpredictable manner to molecular structures.

The liquid crystalline state is governed by weak intermolecular forces, in the order of a few kcal mol^{-1}, and the prediction of bulk properties for a liquid crystal could rely only on a highly accurate description of these interactions. For the simulation of molecular ensembles, Monte Carlo or molecular dynamics calculations have been used, and simulations for simple model liquid crystals have been carried out successfully.[109] Unfortunately, substantial simplifications must be made at the level of the individual molecule to treat the interactions of the ensemble at all. Even with these restrictions, computer times are enormous and the methods are still far from being routine modeling tools. In addition, careful parameterization of the force-field and/or the anisotropic potentials used in the simulation is crucial for reliable results.

On the other hand, classical computational chemistry[110] deals with isolated molecules in the gas phase but allows a very detailed and accurate description of their electronic and geometric structures. The methods range from simple molecular mechanics[111] and semiempirical methods[110] to ab initio[112] and density functional (DFT)[113] theory.

5.1. Shape Analysis

Nematic liquid crystals, as they are used in most LCDs, are rodlike molecules. Deviations from a linear structure towards bent arrangements qualitatively result in a decrease of the clearing temperatures. It is therefore of interest to rapidly form an impression of the three-dimensional shape of novel materials that are candidates for chemical synthesis. In addition, in most cases, there will be conformational flexibility instead of complete rigidity; that is, in the condensed phase at room temperature, the thermal energy available will be sufficient to populate conformers higher in energy than the global minimum. Modeling at the force-field level of theory gives a quick overview of such conformers. For example, four low energy conformers of the bis(1,3-dioxane) **93** (Table 13) are shown in Figure 3.

In addition to these mostly qualitative aspects, it is possible to compute geometrical and electronic structure parameters. From these molecular descriptors, quantitative structure–activity relationships (QSAR)[114] can be derived. This has recently been applied for the prediction of clearing temperatures for a number of liquid crystals.[115] However, the variation in chemical structure must not be too large and the properties of structures not radically different from those used in the training set, otherwise the properties will probably not be predicted correctly.

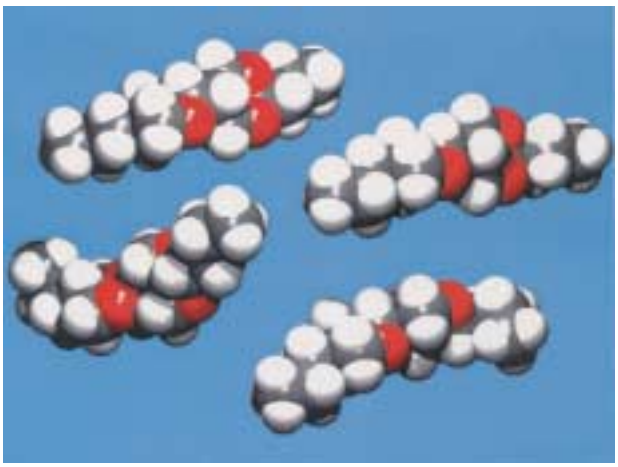

Figure 3. The four lowest energy conformers (within 0.6 kcal mol^{-1}) of the bis(1,3-dioxane) derivative **93**. The global minimum is shown in the upper left corner (MMFF94 force-field calculations).

5.2. Molecular Modeling of Electrooptic Properties

Some of the key parameters for a liquid crystal mixture are the dielectric and optical anisotropies $\Delta\varepsilon$ and Δn. The dielectric anisotropy $\Delta\varepsilon$ is related to molecular properties via the Maier–Meier equation [Eq. (1)][38] and Δn can be obtained from the molecular polarizability α from the Vuks equation [Eq. (4)].[42] The molecular dipole moment μ and the polarizability α can be obtained from a semiempirical, ab initio, or DFT calculation (Figure 4).[116–120]

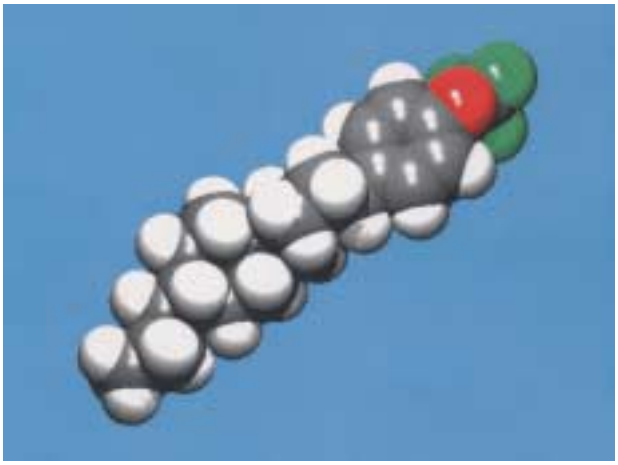

Figure 4. A three-dimensional representation of the liquid crystal CCP-30CF3 **23**. The calculated (AM1) anisotropic polarizabilities are $\alpha_{xx} = 255.7$, $\alpha_{yy} = 153.2$, and $\alpha_{zz} = 159.6$ a.u.; the dipole moments are $\mu_x = 2.95$, $\mu_y = 0.08$, and $\mu_z = 0.52$ D; the angle β towards the orientational axis, approximated by the x axis of the molecule, is 10.0°. The electrooptical anisotropies derived from these values are $\Delta\varepsilon_{AM1} = 5.8$ and $\Delta n_{AM1} = 0.099$. The experimentally determined virtual parameters are 6.9 and 0.087 for $\Delta\varepsilon$ and Δn, respectively. (1 a.u. = 0.14818 Å^3.)

For conformationally flexible molecules, the prediction, especially that of $\Delta\varepsilon$, is somewhat more complicated, since different conformers may possess very different dipole moments even though they are similar in energy. It is then necessary to systematically screen the conformational space and perform a Boltzmann-type weighting of the calculated quantities.

An extreme case in point is the polar terminal group difluoromethoxybenzene. Figure 5 shows three conformers located at the B3LYP/6-311 + G**//B3LYP/6-311 + G** level of theory together with their relative energies and dipole moments. Although these calculations are at an adequate level, their predictive power is rather low. After all, we are dealing with the condensed phase where energy differences of less than 1 kcal mol^{-1} in the gas phase are certainly insignificant. Fortunately, in most cases, there is only one minimum within a few kcal mol^{-1} and the conformer problem disappears.

In order to assess the value of the method, calculations were carried out on a representative test set of liquid crystals that provides a wide range of electrooptical anisotropies. The predicted and experimental electrooptical anisotropies for this set are shown in Figure 6. Only single conformers were used for the calculations.

The influence of the quantum chemical method on the quality of the prediction can easily be checked by moving to higher levels of theory (Figure 7). Hartree – Fock ab initio theory with the split valence 6-31G* basis set is currently the practical limit for molecules the size of liquid crystals. Calculation times for ab initio geometry optimization and polarizability calculations are two to three orders of magnitude longer than those of the AM1 semiempirical method.

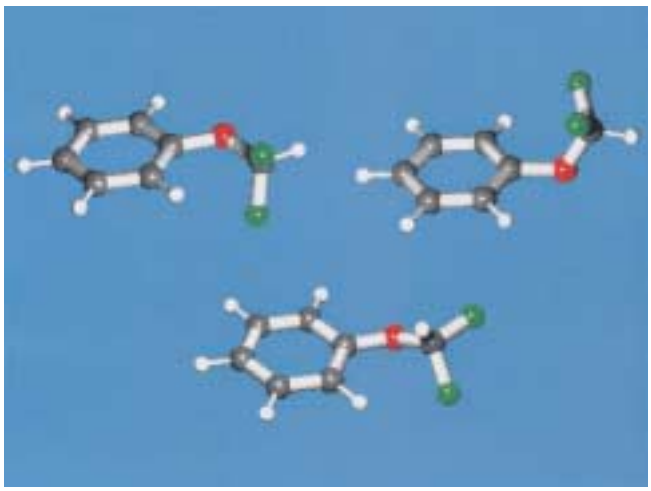

Figure 5. Three low energy conformers of difluoromethoxybenzene at the B3LYP/6-311 + G**//B3LYP/6-311 + G** level of theory: The relative energies and corresponding dipole moments are 0.4 kcal mol^{-1} and 0.98 D (upper left), 0.0 kcal mol^{-1} and 1.12 D (upper right), and 0.1 kcal mol^{-1} and 2.93 D (below).

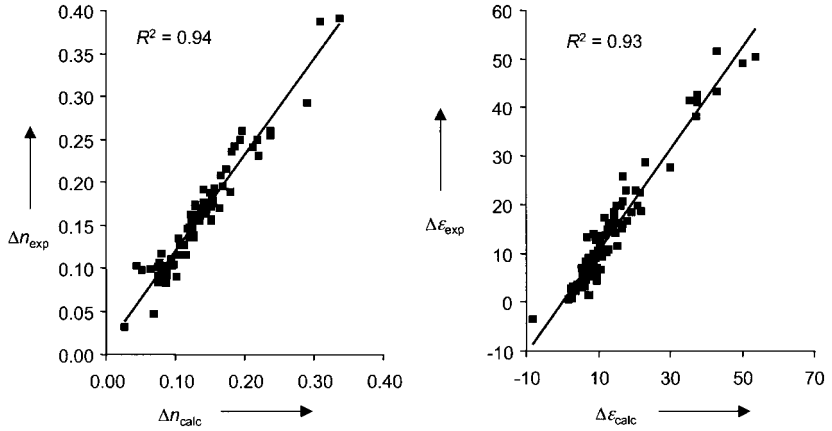

Figure 6. The correlation between semiempirically calculated (AM1) versus extrapolated experimental electrooptical anisotropies (84 samples).

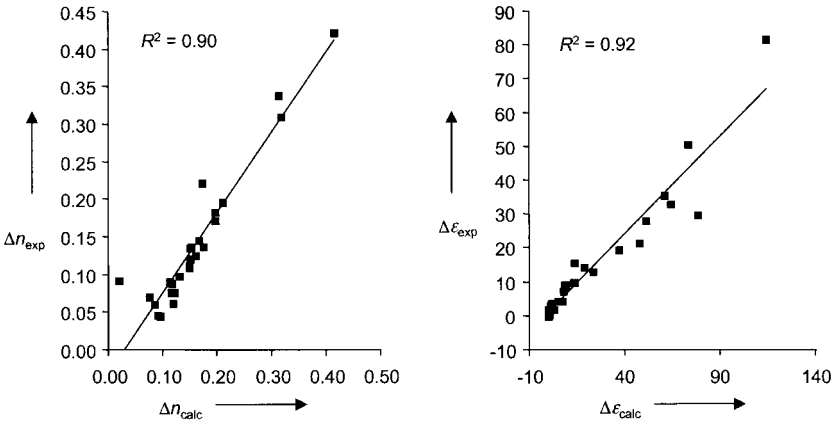

Figure 7. The correlation between ab initio (HF/6-31G*//HF/6-31G*) calculated electrooptical anisotropies versus extrapolated experimental data (26 samples).

Although the ab initio approach is more rigorous theoretically, there is a large systematic overestimation of $\Delta\varepsilon$ and a (smaller) overestimation of Δn. The most likely explanation for this poor performance is the neglect of electron correlation and the use of a too small basis set. It is well known that Hartree – Fock ab initio theory systematically overestimates molecular dipole moments, while DFT and MP2 ab initio and even AM1 reproduce experimentally determined values quite well.[121] Unfortunately, the computational problem cannot be tackled adequately at present. However, the performance of the semiempirical method (which includes some electron correlation effects via the parameterization) is quite satisfactory for standard organic materials, such as most liquid crystals. However, semiempirical theory understandably fails with molecules it was not parameterized for, which became evident with hypervalent sulfur fluorides.[92]

5.3. Modeling-Assisted Prediction of Reliability Parameters

One of the characteristic parameters for the reliability of a liquid crystal mixture is a high VHR value. The VHR of liquid crystal mixtures has been much improved after the introduc-

tion of "superfluorinated materials" (SFMs)[52–54] but there still remains an observable leakage current, which suggests the presence of ions or contamination in the cell.

Modeling the solvation of ions by liquid crystal molecules was supposed to provide a better understanding of the interactions involved and possibly allow predictions regarding the solvation potential of structures not yet synthesized. Many liquid crystals are polar organic materials that possess large dipole moments and lone electron pairs which can interact with ions. In principle, the solvents' macroscopic dielectric constants, dipole moments, and polarizabilities can affect solvation but only a weak correlation with experimental data was found.[122]

For our modeling approach, the semiempirical AM1 method was used because of the relatively large size of liquid crystal molecules. The MOPAC program[120] offers positively charged "artificial elements", the "sparkles", which can be conveniently used to model, for example, alkali metal ions. Sparkles may be regarded as unpolarizable ions of a fixed 1.4 Å diameter. They do not contribute to the orbital count and cannot accept or donate electrons. Since the strongest interactions are expected for positive ions (negative ions are generally larger and their charge is better delocalized) only singly positively charged sparkles were considered. As a suitable measure for the "ion solvation power" of a material, we chose the calculated (AM1) heat of interaction of a liquid crystal molecule with a positive sparkle.

Figure 8 shows the energy of a system consisting of benzonitrile as a simple model liquid crystal and a sparkle as a function of distance.

The calculation shows that there is a steep energy minimum at a nitrogen–sparkle distance of about 3.1 Å and an interaction energy of almost $-11\ \mathrm{kcal\,mol^{-1}}$. The steepness of this energy curve leads to smooth convergence of the geometry optimization: Placing the sparkle in the initial configuration directly over the aromatic ring instead of in the ring plane leads to the same structure after energy minimization.

The geometry of the organic molecule is altered little by the presence of the sparkle; bond lengths change by less than 0.005 Å and bond angles by less than 0.3°. The charge distribution, however, is significantly perturbed by the presence of the charged particle, although the total charge in the organic part of the complex remains zero. A simple valence-bond resonance structure for benzonitrile (Figure 8) illustrates these changes qualitatively but in a strikingly simple manner.

Electron density is easily shifted in the delocalized π-system and this induces an extra dipole moment in addition to the one already present. Thus, the overall effect may best be described as a combination of ion–dipole and ion–induced dipole interactions.

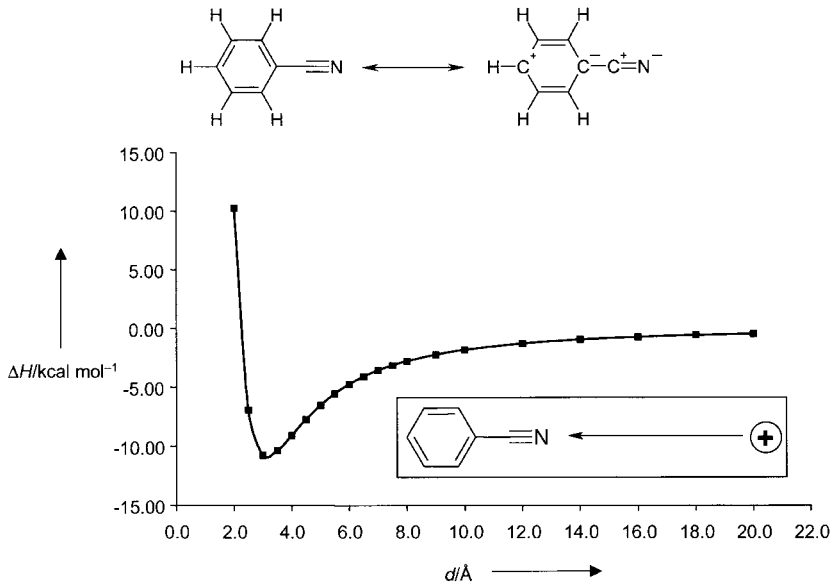

Figure 8. Energy profile for the interaction of a positively charged sparkle with benzonitrile. ΔH denotes the calculated heat of interaction (AM1) and d the distance of the sparkle from the cyano nitrogen atom.

Another case in point, typical for SFM-based materials, is 1,2,3-trifluorobenzene. As for benzonitrile, very little change in molecular geometry is observed but the change in atomic charges is now reduced. Consequently, the heat of interaction is only $-4.4\ \mathrm{kcal\,mol^{-1}}$, which implies a smaller solvation power. It is well known, that for active matrix applications, nitriles are not suitable because of poor voltage-holding behavior. The empirical and perhaps initially puzzling finding, that only the recently introduced SFMs are suitable for active matrix displays, is nicely corroborated by this simple model of ion solvation.

Finally, instead of the model systems discussed so far, a set of complete liquid crystals for TN, as well as AMD, applications was used. Immediately, the problem of more than one polar group in a given molecule arises. For example, in esters of the type shown in Figure 9, the sparkle may interact with the ester group (a) or with the terminal nitrile (b).

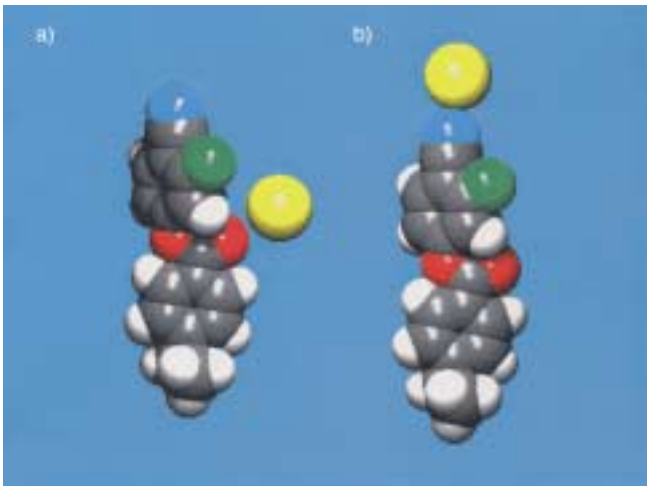

Figure 9. Two local minima for the interaction of a positive sparkle (yellow) with the liquid crystal ME2N.F (**132**).

Both structures are energy minima but the heat of interaction with the nitrile group is -12.6 kcal mol^{-1}, whereas, with the ester carbonyl group (a) it is only -8.0 kcal mol^{-1}. Under equilibrium conditions, only structure (b) will exist and (a) can be safely neglected. In a similar way, the structures and energies of other typical liquid crystals were calculated and the data are shown in Figure 10.

Although in essence a very simple electrostatic model is used, the results are often counterintuitive: The calculated heats of interaction do not necessarily have a direct relationship with the dipole moment or the polarizability; for example, the computed dipole moment is 7.1 D for ME2N.F but "only" 3.9 D for PCH-3 and 3.1 D for CCP-3OCF3 **23**. Admittedly qualitative in nature, this simple model allows a preliminary assessment of the AMD suitability of new liquid crystals before their actual synthesis.

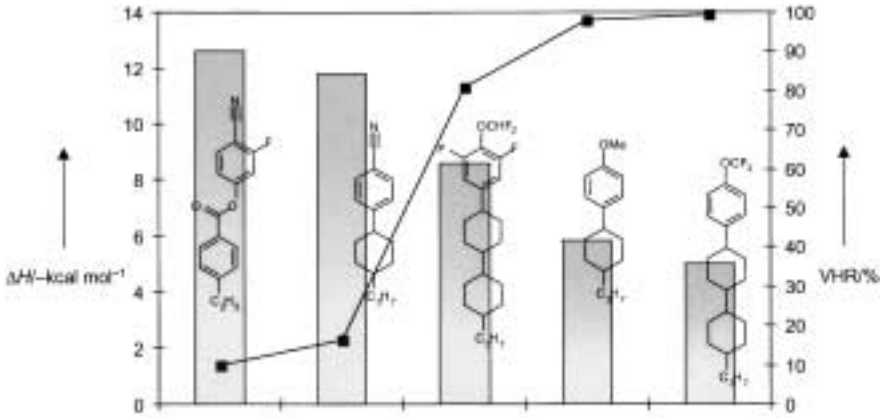

Figure 10. Calculated (AM1) heats of interaction (ΔH) and voltage-holding ratios (VHR) for some typical liquid crystals.

6. Conclusion and Outlook

During the time span between their first application in simple LCDs and their use in modern AM-LCDs, structural as well as physicochemical characteristics of liquid crystalline materials have changed drastically. The parallel development of various types of active matrix technologies, with their sometimes very different demands with regard to the physical properties of the materials, led to a broad diversification of the chemical structures and also of the synthetic methods used for their production on an industrial scale.

The increasing pace of the technological advance in the display field has created a powerful incentive for the materials manufacturers to put the design and development of new liquid crystals on a more rational basis. Although it might not be expected offhand, some important properties of the condensed liquid crystalline phase can be predicted by modeling the isolated molecules. There are relationships between molecular parameters and experimental clearing temperatures, electrooptical anisotropies can routinely be calculated for any structure, and a simple model for the solvation of ions yields results in agreement with important liquid crystal reliability parameters like VHR or residual DC. In addition to these properties specific to liquid crystals, modeling offers important tools for the synthetic organic chemist to guide synthetic strategies by providing information on conformational space, thermodynamic stabilities, activation energies, and the ground-state and transition structures of molecules.

A decisive driving force for the future development of new AM-LCD technologies will be cost reduction in mass production. The reduction of the power consumption, such as by use of reflective displays, will be another important goal. Within the next few years, the consumer will have to choose from a broad spectrum of different devices based on AM-LCDs, ranging from large screens for TV applications to very small displays with increased resolution for viewfinders, mobile phones, or virtual reality goggles. For the design of liquid crystals, the challenge to explore materials with extreme electrooptical and viscoelastic properties will continue, with ever more stringent quality requirements than currently required.

Received: July 16, 1999
Revised: May 4, 2000 [A 353]

[1] Source: Stanford Resources, Inc. Further information is available in the internet: http://www.webcom.com/sr/.
[2] S. Kobayashi, H. Hori, Y. Tanaka in *Active Matrix Liquid Crystal Displays* in *Handbook of Liquid Crystal Research* (Eds.: P. J. Collings, J. S. Patel), Oxford University Press, New York, **1997**, pp. 415–444.
[3] K. Nakao, *EKISHO J. Jpn. Liq. Cryst. Soc.* **1999**, *3*, 62–63.
[4] Merck KGaA, internal estimate.
[5] M. Schadt, W. Helfrich, *Appl. Phys. Lett.* **1971**, *18*, 127.
[6] F. Reinitzer, *Monatsh. Chem.* **1888**, *9*, 421.
[7] O. Lehmann, *Flüssige Kristalle, sowie Plastizität von Kristallen im Allgemeinen, molekulare Umlagerungen und Aggregatzustandsänderungen*, Engelmann, Leipzig, **1904**.
[8] a) P. G. de Gennes, J. Prost, *The Physics of Liquid Crystals*, Oxford University Press, London, **1993**; b) W. H. de Jeu, *Physical Properties of Liquid Crystalline Materials*, Gordon and Breach, New York, **1980**.
[9] D. Demus, H. Demus, H. Zaschke, *Flüssige Kristalle in Tabellen*, VEB Deutscher Verlag für Grundstoffindustrie, Leipzig, **1974**.
[10] D. Demus, L. Richter, *Textures of Liquid Crystals*, Verlag Chemie, Weinheim, **1978**.
[11] *Handbook of Liquid Crystals* (Eds.: D. Demus, J. Goodby, G. W. Gray, H.-W. Spiess, V. Vill), WILEY-VCH, Weinheim, **1998**.
[12] V. Vill, *LiqCryst 3.1—Databases of Liquid Crystalline Compounds*, LCI Publisher GmbH, Hamburg, **1998**.
[13] a) General review: G. Solladié, R. G. Zimmermann, *Angew. Chem.* **1984**, *96*, 335–349; *Angew. Chem. Int. Ed. Engl.* **1984**, *23*, 348–362; b) Technical applications: D. Pauluth, A. E. F. Wächtler in *Synthesis and Application of Chiral Liquid Crystals* in *Chirality in Industry, Vol. II* (Eds.: A. N. Collins, G. N. Sheldrake, J. Crosby), Wiley, New York, **1997**, pp. 264–285.
[14] a) G. W. Gray, K. J. Harrison (Ministry of Defense, Great Britain), GB-B 1433130, **1972** [*Chem. Abstr.* **1974**, *81*, 96988]; b) G. W. Gray, K. J. Harrison, J. A. Nash, *Electron. Lett.* **1973**, *9*, 130.
[15] R. Eidenschink, D. Erdmann, J. Krause, L. Pohl, *Angew. Chem.* **1977**, *89*, 103; *Angew. Chem. Int. Ed. Engl.* **1977**, *16*, 100.
[16] D. Demus, H.-J. Deutscher, F. Kuschel, H. Schubert (VEB Werk für Fernsehelektronik), DE-B 2429093, **1975** [*Chem. Abstr.* **1977**, *89*, 129118].
[17] R. Eidenschink, D. Erdmann, J. Krause, L. Pohl, *Angew. Chem.* **1978**, *90*, 133; *Angew. Chem. Int. Ed. Engl.* **1978**, *17*, 133.

[18] R. Eidenschink, G. Haas, M. Römer, B. S. Scheuble, *Angew. Chem.* **1984**, *96*, 151; *Angew. Chem. Int. Ed. Engl.* **1984**, *23*, 147.

[19] P. Kirsch, V. Reiffenrath, M. Bremer, *Synlett* **1999**, 389 – 396.

[20] For historical overviews of the materials development for all types of LCDs: a) T. Inukai, K. Miyazawa, *EKISHO J. Jpn. Liq. Cryst. Soc.* **1997**, *1*, 9 – 22; b) R. Eidenschink, *Kontakte (Darmstadt)* **1979**, (1), 15 – 18.

[21] a) "Applications: TN, STN Displays": H. Hirschmann, V. Reiffenrath in *Handbook of Liquid Crystals*, *Vol. 2A* (Eds.: D. Demus, J. Goodby, G. W. Gray, H.-W. Spiess, V. Vill), WILEY-VCH, Weinheim, **1998**, pp. 199 – 229; b) B. S. Scheuble, *Kontakte (Darmstadt)* **1989**, (1), 34 – 48; c) P. M. Alt, P. Pleshko, *IEEE Trans. Electron Devices* **1974**, *ED-21*, 146 – 155.

[22] T. J. Scheffer, J. Nehring, M. Kaufmann, H. Amstutz, D. Heimgartner, P. Eglin, *SID Dig. Tech. Pap.* **1985**, *16*, 120 – 123.

[23] a) R. Williams, *J. Chem. Phys.* **1963**, *39*, 384; b) R. Williams (RCA), US-A 3322485, **1962** [*Chem. Abstr.* **1968**, *68*, 34254].

[24] G. H. Heilmeier, L. A. Zanoni, L. A. Barton, *Appl. Phys. Lett.* **1968**, *13*, 46.

[25] B. J. Lechner, *Proc. IEEE* **1971**, *59*, 1566.

[26] T. P. Brody, J. A. Asars, G. D. Dixon, *IEEE Trans. Electron Devices* **1973**, *ED-20*, 995.

[27] D. R. Baraff, J. R. Long, *IEEE Trans. Electron Devices* **1973**, *ED-20*, 995.

[28] a) U. Finkenzeller, *Spektrum Wiss.* **1990**, (8), 55 – 62; b) D. Pauluth, T. Geelhaar, *Nachr. Chem. Tech. Lab.* **1997**, *45*, 9 – 15.

[29] a) K. H. Yang, *Int. Dev. Res. Cent. Techn. Rep. IDRC* **1991**, 68; b) Y. Iimura, S. Kobayashi, T. Sugiyama, Y. Toko, T. Hashimoto, K. Katoh, *SID Dig. Tech. Pap.* **1994**, 915; c) T. Sugiyama, Y. Toko, T. Hashimoto, K. Kato, Y. Iimura, S. Kobayashi, *SID Dig. Tech. Pap.* **1994**, 919; d) M. Schadt, H. Seiberle, A. Schuster, S. M. Kelly, *Jpn. J. Appl. Phys.* **1995**, *34*, 764.

[30] a) R. Kiefer, B. Weber, F. Winscheid, G. Baur, *Proceedings of the 12th International Display Research Conference* (Hiroshima, Japan), **1992**, 547 (Society of Information Display and the Institute of Television Engineers of Japan); b) M. Oh-e, K. Kondo, *Liq. Cryst.* **1997**, *22*, 379 – 390, and references therein.

[31] A. Takeda, *EKISHO J. Jpn. Liq. Cryst. Soc.* **1999**, *3*, 117 – 123.

[32] a) M. Matsuura, *EKISHO J. Jpn. Liq. Cryst. Soc.* **1997**, *1*, 23 – 32; b) M. Hayashi, A. Seki, T. Togawa, *SID Dig. Tech. Pap.* **1997**, 383.

[33] a) W. Maier, A. Saupe, *Z. Naturforsch. A* **1959**, *14*, 882; b) W. Maier, A. Saupe, *Z. Naturforsch. A* **1960**, *15*, 287.

[34] S. Marcelja, *J. Chem. Phys.* **1974**, *60*, 3599.

[35] J. G. J. Ypma, G. Vertogen, H. T. Koster, *Mol. Cryst. Liq. Cryst.* **1976**, *37*, 57.

[36] W. H. de Jeu, J. van der Veen, *Mol. Cryst. Liq. Cryst.* **1977**, *40*, 1.

[37] U. Finkenzeller, *Kontakte (Darmstadt)* **1988**, (2), 7 – 14.

[38] In Equation (1), k_B denotes the Boltzmann constant, S the Saupe orientational order parameter of the nematic phase,[23] F the reaction field factor $\left(F = \frac{1}{1-f\alpha}; f = \frac{\varepsilon-1}{2\pi\varepsilon_0 a^3(2\varepsilon+1)}\right)$, and h the cavity factor $\left(h = \frac{3\varepsilon}{2\varepsilon+1}\right)$. For ε, the macroscopic dielectric constant is used: a) W. Maier, G. Meier, *Z. Naturforsch. A* **1961**, *16*, 262 – 267; b) D. Demus, G. Pelzl, *Z. Chem.* **1982**, *21*, 1; c) J. Michl, E. W. Thulstrup, *Spectroscopy with Polarized Light: Solute Alignment by Photoselection, in Liquid Crystals, Polymers, and Membranes*, VCH, Weinheim, **1995**, pp. 171 – 221.

[39] C. Mauguin, *Bull. Soc. Fr. Mineral.* **1911**, *34*, 71 – 117.

[40] a) C. A. Gooch, H. A. Tarry, *Electron. Lett.* **1974**, *10*, 2 – 4; b) C. A. Gooch, H. A. Tarry, *J. Phys. D* **1975**, *8*, 1575 – 1584.

[41] a) L. Pohl, R. Eidenschink, F. del Pino, G. Weber (Merck KGaA), US-A 4285829, **1979** [*Chem. Abstr.* **1980**, *92*, 207152]; b) L. Pohl, G. Weber, R. Eidenschink, G. Baur, W. Fehrenbach, *Appl. Phys. Lett.* **1981**, *38*, 497 – 499.

[42] M. F. Vuks, *Opt. Spectrosc. (Engl. Transl.)* **1966**, *20*, 361.

[43] a) J. L. Ericksen, *Trans. Soc. Rheol.* **1961**, *5*, 23; b) F. M. Leslie, *Arch. Ration. Mech. Anal.* **1968**, *28*, 265; c) A. Raviol, W. Stille, G. Strobl, *J. Chem. Phys.* **1995**, *103*, 3788 – 3794.

[44] M. Bremer, S. Naemura, K. Tarumi, *Jpn. J. Appl. Phys.* **1998**, *37*, L88 – L90.

[45] T. Jacob, E. Böhm, K. Tarumi, *SID Dig. Tech. Pap.* **1996**, 131.

[46] a) A. Sasaki, T. Uchida, S. Miyagami, *Japan Display* **1986**, 62; b) M. Schadt, *Displays* **1992**, *13*, 11.

[47] Y. Nakazono, H. Ichinose, A. Sawada, S. Naemura, M. Bremer, K. Tarumi, *Int. Dev. Res. Cent. Techn. Rep. IDRC* **1997**, 65.

[48] S. Nagata, E. Takeda, Y. Nanno, T. Kawaguchi, Y. Mino, A. Otsuka, S. Ishihara, *SID Dig. Tech. Pap.* **1989**, 242.

[49] S. Naemura, Y. Nakazono, H. Ichinose, A. Sawada, E. Böhm, M. Bremer, K. Tarumi, *SID Dig. Tech. Pap.* **1997**, 199.

[50] N. Fukuoka, M. Okamoto, Y. Yamamoto, M. Hasegawa, Y. Tanaka, H. Hatoh, K. Mukai, *AM LCD* **1994**, 216.

[51] G. Weber, U. Finkenzeller, T. Geelhaar, H. J. Plach, B. Rieger, L. Pohl, *Liq. Cryst.* **1989**, *5*, 1381 – 1388.

[52] Y. Goto, T. Ogawa, S. Sawada, S. Sugimori, *Mol. Cryst. Liq. Cryst.* **1991**, *209*, 1 – 7.

[53] K. Tarumi, M. Bremer, B. Schuler, *IEICE Trans. Electron.* **1996**, *E79-C*, 1035 – 1039.

[54] K. Tarumi, M. Bremer, T. Geelhaar, *Annu. Rev. Mater. Sci.* **1997**, *27*, 423 – 441.

[55] F. Mongin, R. Maggi, M. Schlosser, *Chimia* **1996**, *50*, 650 – 652, and references therein.

[56] a) T. Hayashi, M. Konishi, Y. Kobori, M. Kumada, T. Higuchi, K. Hirotsu, *J. Am. Chem. Soc.* **1984**, *106*, 158; b) E. Negishi, *Acc. Chem. Res.* **1982**, *15*, 340; c) P. L. Castle, D. A. Widdowson, *Tetrahedron Lett.* **1986**, *49*, 6013; d) R. Arnek, K. Zetterberg, *Organometallics* **1987**, 1230.

[57] For reviews on various types of palladium-mediated C–C coupling reactions, see the special issue: *J. Organomet. Chem.* **1999**, *576*, 1 – 317.

[58] E. Poetsch, *Kontakte (Darmstadt)* **1988**, (2), 15 – 28.

[59] a) C. Petrier, J. C. de Souza Barboza, C. Dupuy, J. L. Luche, *J. Org. Chem.* **1985**, *50*, 5761; b) C. Petrier, J. L. Luche, C. Dupuy, *Tetrahedron Lett.* **1984**, 3463.

[60] a) K. Tamoa, K. Sumitani, M. Kumada, *J. Am. Chem. Soc.* **1972**, *94*, 4374; b) K. Tamoa, K. Sumitani, M. Kumada, *J. Am. Chem. Soc.* **1972**, *94*, 9268; c) R. J. P. Couriu, J. P. Masse, *J. Chem. Soc. Chem. Commun.* **1972**, 144; d) A. Sekiya, N. Ishikawa, *J. Organomet. Chem.* **1976**, *118*, 349; e) G. W. Parshall, J. *Am. Chem. Soc.* **1974**, *96*, 2360.

[61] M. Miyaura, A. Suzuki, *J. Chem. Soc. Chem. Commun.* **1979**, 866.

[62] J. March, *Advanced Organic Chemistry*, 3rd ed., Wiley, New York, **1985**, pp. 845 – 854.

[63] R. F. Heck, *Org. React.* **1982**, *27*, 345.

[64] V. Reiffenrath, U. Finkenzeller, E. Poetsch, B. Rieger, D. Coates, *SPIE Liq. Cryst. Displays Appl.* **1990**, *1257*, 84 – 94.

[65] The phase transition temperatures are given in °C, the γ_1 values in mPa s. Phase abbreviations are C = crystalline, S_x = smectic X, N = nematic, I = isotropic. Usually, $T_{NI,extr}$, $\Delta\varepsilon$, Δn, and γ_1 were determined by linear extrapolation from a 10% w/w solution in the commercially available Merck mixture ZLI-4792 ($T_{NI} = 92.8\,°C$, $\Delta\varepsilon = 5.3$, $\Delta n = 0.0964$). The extrapolated values are corrected empirically for differences in the order parameter. In some marked cases, the following mixtures were used for extrapolation: ZLI-2857 ($T_{NI} = 82.3\,°C$, $\Delta\varepsilon = -1.4$, $\Delta n = 0.0776$), ZLI-3086 ($T_{NI} = 72.0\,°C$, $\Delta\varepsilon = 0.1$, $\Delta n = 0.1131$), and ZLI-1132 ($T_{NI} = 71.0\,°C$, $\Delta\varepsilon = 12.8$, $\Delta n = 0.1406$). For the pure substances, the mesophases were identified by optical microscopy and the phase transition temperatures by differential scanning calorimetry.

[66] a) E. Bartmann, *Ber. Bunsenges. Phys. Chem.* **1993**, *97*, 1349 – 1355; b) J. C. Liang, S. Kumar, *Mol. Cryst. Liq. Cryst.* **1987**, *142*, 77 – 84; c) J. C. Liang, J. O. Cross, L. Chen, *Mol. Cryst. Liq. Cryst.* **1989**, *147*, 199 – 206.

[67] For general methods for the synthesis of similar substances, see: a) L. N. Markovskij, V. E. Pashinnik, A. V. Kirsanov, *Synthesis* **1973**, 787 – 789; b) N. Yoshino, M. Kitamura, T. Seto, Y. Shibata, M. Abe, K. Ogino, *Bull. Chem. Soc. Jpn.* **1992**, *65*, 2141 – 2144; c) B. Betzemeier, P. Knochel, *Angew. Chem.* **1997**, *109*, 2736 – 2738; *Angew. Chem. Int. Ed. Engl.* **1997**, *36*, 2623 – 2624.

[68] V. Reiffenrath, H. A. Kurmeier, E. Poetsch, H. Plach, U. Finkenzeller, E. Bartmann, J. Krause, B. Scheuble, D. Dorsch, G. Weber (Merck KGaA), EP-B 441932, **1991** [*Chem. Abstr.* **1996**, *125*, 208555].

[69] A. I. Pavluchenko, N. I. Smirnova, V. F. Petrov, Yu. A. Fialkov, S. V. Shelyazhenko, L. M. Yagupolskii, *Mol. Cryst. Liq. Cryst.* **1991**, *209*, 225 – 235.

[70] S. V. Shelyazhenko, Yu. A. Fialkov, L. M. Yagupolskii, *J. Org. Chem. USSR (Engl. Transl.)* **1992**, *28*, 1317 – 1324; *Zh. Org. Khim.* **1992**, *28*, 1652 – 1660.

[71] a) G. A. Olah, T. Yamato, T. Hashimoto, J. G. Shih, N. Trivedi, B. P. Singh, M. Piteau, J. A. Olah, *J. Am. Chem. Soc.* **1987**, *109*, 3708 – 3713. Different syntheses for trifluoromethoxy derivatives are reported in: b) M. R. Pavia, S. J. Lobbestael, D. Nugiel, D. R. Mayhugh, V. E. Gregor, *J. Med. Chem.* **1992**, *35*, 4238 – 4248; c) M. Kuroboshi, K. Suzuki, T. Hiyama, *Tetrahedron Lett.* **1992**, *29*, 4173 – 4176; d) W. A. Sheppard, *J. Org. Chem.* **1964**, *29*, 1 – 11.

[72] Analogous to: D. C. England, L. R. Melby, M. A. Dietrich, R. V. Lindsey, Jr., *J. Am. Chem. Soc.* **1960**, *82*, 5116 – 5122.

[73] W. A. Sheppard, *J. Org. Chem.* **1964**, *29*, 1 – 11.

[74] M. Schadt, R. Buchecker, A. Villiger, *Liq. Cryst.* **1990**, *7*, 519 – 536.

[75] Review: S. M. Kelly, *Liq. Cryst.* **1996**, *20*, 493 – 515.

[76] M. Petrzilka, *Mol. Cryst. Liq. Cryst.* **1985**, *131*, 109 – 123.

[77] R. Eidenschink, *Mol. Cryst. Liq. Cryst.* **1983**, *94*, 119 – 129.

[78] R. Eidenschink, *Mol. Cryst. Liq. Cryst.* **1985**, *123*, 57 – 75.

[79] a) M. A. Osman, *Mol. Cryst. Liq. Cryst.* **1985**, *128*, 45 – 63; b) P. Balkwill, D. Bishop, A. Pearson, I. Sage, *Mol. Cryst. Liq. Cryst.* **1985**, *123*, 1 – 13; c) J. E. Fearon, G. W. Gray, A. D. Ifill, K. J. Toyne, *Mol. Cryst. Liq. Cryst.* **1985**, *124*, 89 – 103.

[80] D. Demus, Y. Goto, S. Sawada, E. Nakagawa, H. Saito, R. Tarao, *Mol. Cryst. Liq. Cryst.* **1995**, *260*, 1 – 21.

[81] G. W. Gray, M. Hird, D. Lacey, K. J. Toyne, *Mol. Cryst. Liq. Cryst.* **1989**, *172*, 165 – 189.

[82] E. Bartmann, D. Dorsch, U. Finkenzeller, *Mol. Cryst. Liq. Cryst.* **1991**, *204*, 77 – 89.

[83] E. Bartmann, J. Krause, K. Tarumi, *23nd Freiburger Arbeitstagung Flüssigkristalle* (Freiburg, Germany), **1994**.

[84] E. Bartmann, U. Finkenzeller, E. Poetsch, V. Reiffenrath, K. Tarumi, *22nd Freiburger Arbeitstagung Flüssigkristalle* (Freiburg, Germany), **1993**.

[85] M. Hird, K. J. Toyne, A. J. Slaney, J. W. Goodby, G. W. Gray, *J. Chem. Soc. Perkin Trans. 2* **1993**, 2337 – 2349.

[86] P. Kirsch, K. Tarumi, *Angew. Chem.* **1998**, *110*, 501 – 506; *Angew. Chem. Int. Ed.* **1998**, *37*, 484 – 489.

[87] R. Eidenschink, L. Pohl, M. Römer, B. Scheuble (Merck KGaA), EP-B 107759, **1984** [*Chem. Abstr.* **1984**, *101*, 63770].

[88] a) E. Bartmann, *Adv. Mater.* **1996**, *8*, 570 – 573; b) E. Bartmann, K. Tarumi (Merck KGaA), DE-B 19531165, **1995** [*Chem. Abstr.* **1996**, *124*, 328585]; c) T. Ando, K. Shibata, S. Matsui, K. Miyazawa, H. Takeuchi, Y. Hisatsune, F. Takeshita, E. Nakagawa, K. Kobayashi, Y. Tomi (Chisso Corp.), EP-B 0844229, **1998** [*Chem. Abstr.* **1998**, *129*, 60620].

[89] A. Haas, M. Spitzer, M. Lieb, *Chem. Ber.* **1988**, *121*, 1329 – 1340.

[90] a) H.-M. Vorbrodt, J. Vogel, H. Zaschke, G. Pelzl, D. Demus, *Mol. Cryst. Liq. Cryst.* **1985**, *123*, 137 – 141; b) C. Tschierske, H. Altmann, H. Zaschke, G. Brezesinski, F. Kuschel, *Mol. Cryst. Liq. Cryst.* **1990**, *191*, 295 – 300.

[91] V. S. Bezborodov, V. F. Petrov, V. I. Lapanik, *Liq. Cryst.* **1996**, *20*, 785 – 796.

[92] P. Kirsch, M. Bremer, M. Heckmeier, K. Tarumi, *Angew. Chem.* **1999**, *111*, 2174 – 2178; *Angew. Chem. Int. Ed.* **1999**, *38*, 1989 – 1992.

[93] a) W. A. Sheppard, *J. Am. Chem. Soc.* **1960**, *82*, 4751 – 4752; b) W. A. Sheppard, *J. Am. Chem. Soc.* **1962**, *84*, 3064 – 3071; c) W. A. Sheppard, *J. Am. Chem. Soc.* **1962**, *84*, 3072 – 3076.

[94] M. P. Greenhall, *15th International Symposium on Fluorine Chemistry* (Vancouver, Canada), **1997**, presentation FRx C-2.

[95] a) H. Okumura, *EKISHO J. Jpn. Liq. Cryst. Soc.* **1999**, *3*, 17 – 24; b) P. Raynes, *28th Freiburger Arbeitstagung Flüssigkristalle* (Freiburg, Germany), **1999**.

[96] V. Reiffenrath, R. Hittich, M. Kompter, G. Weber, H. A. Kurmeier, H. Plach, E. Poetsch (Merck KGaA), EP-B *418362*, **1991** [*Chem. Abstr.* **1991**, *114*, 228424].

[97] a) P. Kirsch, E. Poetsch, *Adv. Mater.* **1998**, *10*, 602 – 606; b) E. Poetsch, W. Binder, J. Krause, K. Tarumi (Merck KGaA), DE-B 19525314, **1995** [*Chem. Abstr.* **1997**, *126*, 150650]; c) R. Buchecker, G. Marck, A. Villiger (Hoffmann – La Roche AG), EP-B 0732330, **1995** [*Chem. Abstr.* **1996**, *125*, 343068].

[98] Preparation analogous to: W. Dmowski, R. A. Kolinski, *Rosz. Chem.* **1974**, *48*, 1697 – 1706.

[99] K. Kanie, Y. Tanaka, M. Shimizu, S. Takehara, T. Hiyama, *Chem. Lett.* **1997**, 827 – 828.

[100] J. Fried, S. Kittisopikul, E. A. Hallinan, *Tetrahedron Lett.* **1984**, *25*, 4329.

[101] R. Noyori, S. Murata, M. Suzuki, *Tetrahedron* **1981**, *37*, 3899.

[102] S. Sugimori, T. Kojima (Chisso Corp.), EP-B 0084974, **1983** [*Chem. Abstr.* **1984**, *100*, 15786].

[103] K. Ohmuro, S. Kataoka, T. Sasaki, Y. Koike, *SID Dig. Tech. Pap.* **1997**, 845.

[104] P. Kirsch, A. Ruhl, R. Sander, J. Krause, K. Tarumi (Merck KGaA), DE-B 19714231, **1998** [*Chem. Abstr.* **1998**, *129*, 296532].

[105] P. Kirsch, K. Tarumi, *Liq. Cryst.* **1999**, *26*, 449 – 452.

[106] V. Reiffenrath, J. Krause, H. J. Plach, G. Weber, *Liq. Cryst.* **1989**, *5*, 159 – 170.

[107] G. A. Olah, J. T. Welch, Y. D. Vankar, M. Nojima, I. Kerekes, J. A. Olah, *J. Org. Chem.* **1979**, *44*, 3872 – 3881.

[108] M. Bremer, *Adv. Mater.* **1995**, *7*, 867.

[109] a) For a general overview on computer simulation of liquid crystals, see: "Theory of the Liquid Crystalline State: Molecular Modelling": M. R. Wilson in *Handbook of Liquid Crystals*, *Vol. 1* (Eds.: D. Demus, J. Goodby, G. W. Gray, H.-W. Spiess, V. Vill), WILEY-VCH, Weinheim, **1998**, p. 72; "Computer Simulation of Liquid Crystal Phases Formed by Gay – Berne Mesogens": b) M. A. Bates, G. R. Luckhurst in *Liquid Crystals I* (Ed.: D. M. P. Mingos), Springer, Heidelberg, **1999**, p. 65.

[110] T. Clark, *A Handbook of Computational Chemistry*, Wiley, New York, **1985**.

[111] U. Burkert, N. L. Allinger, *Molecular Mechanics*, ACS Monograph 177, American Chemical Society, Washington, DC, **1982**.

[112] W. J. Hehre, L. Radom, P. von R. Schleyer, J. A. Pople, *Ab Initio Molecular Orbital Theory*, Wiley, New York, **1986**.

[113] W. Kohn, A. D. Becke, R. G. Parr, *J. Phys. Chem.* **1996**, *100*, 12974 – 12980.

[114] M. Karelson, V. S. Lobanov, A. R. Katrizky, *Chem. Rev.* **1996**, *96*, 1027 – 1043.

[115] S. R. Johnson, P. C. Jurs, *Chem. Mater.* **1999**, *11*, 1007 – 1023.

[116] M. Bremer, K. Tarumi, *Adv. Mater.* **1993**, *5*, 842 – 848.

[117] M. Klasen, M. Bremer, A. Götz, A. Manabe, S. Naemura, K. Tarumi, *Jpn. J. Appl. Phys.* **1998**, *37*, L945-L948.

[118] SPARTAN Version 5.1, *Wavefunction Inc.*, Irvine, CA.

[119] *Gaussian 98, Revision A.6*: M. J. Frisch, G. W. Trucks, H. B. Schlegel, G. E. Scuseria, M. A. Robb, J. R. Cheeseman, V. G. Zakrzewski, J. A. Montgomery, Jr., R. E. Stratmann, J. C. Burant, S. Dapprich, J. M. Millam, A. D. Daniels, K. N. Kudin, M. C. Strain, O. Farkas, J. Tomasi, V. Barone, M. Cossi, R. Cammi, B. Mennucci, C. Pomelli, C. Adamo, S. Clifford, J. Ochterski, G. A. Petersson, P. Y. Ayala, Q. Cui, K. Morokuma, D. K. Malick, A. D. Rabuck, K. Raghavachari, J. B. Foresman, J. Cioslowski, J. V. Ortiz, B. B. Stefanov, G. Liu, A. Liashenko, P. Piskorz, I. Komaromi, R. Gomperts, R. L. Martin, D. J. Fox, T. Keith, M. A. Al-Laham, C. Y. Peng, A. Nanayakkara, C. Gonzalez, M. Challacombe, P. M. W. Gill, B. Johnson, W. Chen, M. W. Wong, J. L. Andres, C. Gonzalez, M. Head-Gordon, E. S. Replogle, J. A. Pople, *Gaussian, Inc.*, Pittsburgh, PA, **1998**.

[120] *MOPAC V6.0*, QCPE 455, Indiana University, Bloomington, IN.

[121] A. Klamt, V. Jonas, T. Bürger, J. C. W. Lohrenz, *J. Phys. Chem.* **1998**, *102*, 5074 – 5085.

[122] C. Reichardt, *Chem. Rev.* **1994**, *94*, 2319 – 2358.